

Geometry of multidimensional Farey summation algorithm and frieze patterns

Oleg Karpenkov and Matty van Son

October 18, 2024

Abstract

In this paper we develop a new geometric approach to subtractive continued fraction algorithms in high dimensions. We adapt a version of Farey summation to the geometric techniques proposed by F. Klein in 1895. More specifically we introduce Farey polyhedra and their sails that generalise respectively Klein polyhedra and their sails, and show similar duality properties of the Farey sail integer invariants. The construction of Farey sails is based on the multidimensional generalisation of the Farey tessellation provided by a modification of the continued fraction algorithm introduced by R. W. J. Meester. We classify Farey polyhedra in the combinatorial terms of prismatic diagrams. Prismatic diagrams extend boat polygons introduced by S. Morier-Genoud and V. Ovsienko in the two-dimensional case. As one of the applications of the new theory we get a multidimensional version of Conway-Coxeter frieze patterns. We show that multidimensional frieze patterns satisfy generalised Ptolemy relations.

Contents

1	Introduction	2
1.1	History and background	2
1.2	Main results	4
2	Farey tessellation and related algorithms	6
2.1	A few words on integer geometry	6
2.2	Farey tessellation in higher dimensions	6
2.2.1	Construction of the Farey tessellation	6
2.2.2	Farey and quasi-Farey nets	8
2.3	Description of the Farey summation algorithm	9
2.4	Definition of Farey summation continued fractions	11
2.4.1	Enumeration of vertices	11
2.4.2	Tabulation of the algorithm	11
2.5	Meester algorithm	12
2.5.1	A general definition	12
2.5.2	Extended Meester algorithm continued fraction	14
2.5.3	Reconstruction of Farey simplices for a given continued fraction	15

Keywords: Farey tessellation, frieze patterns, subtractive algorithms, multidimensional continued fractions, lattice geometry, triangulated polyhedra

2.6	A few words on convergence of the Farey summation algorithm	16
2.6.1	The divergence set is everywhere dense	16
2.6.2	No guaranteed algebraic cubic periodicity of the Farey summation algorithm	17
3	Properties and invariants of Farey polyhedra	17
3.1	Basic properties of Farey tessellation	18
3.2	Prismatic triangulations	19
3.2.1	Ordered path-triangulations and their complete invariant	19
3.2.2	Decks, masts, yards, crow's nests, and pennants	19
3.2.3	Prismatic polygons and diagrams	20
3.2.4	Prismatic flag diagrams	23
3.2.5	Canonical Prismatic flag diagrams and Farey summation continued fractions	23
3.3	Sails and their LLS sequences	24
3.3.1	Sails of prismatic diagrams and Farey polyhedra	24
3.3.2	On the masts at the point of dimension drop	25
3.3.3	A rigid structure of Farey masts, nose stretching	25
3.3.4	LLS-sequences and their dualities	26
3.4	Semi-group of matrices by multiplication	29
3.4.1	Matrices associated to the steps of the algorithm	29
3.4.2	Partial quotients	29
3.5	LLS-sequence in the three-dimensional case	31
3.5.1	Values of integer sines in the LLS-sequence	31
3.5.2	Integer arctangent of cones in three dimensions and sails	32
3.5.3	Application to sails	33
3.6	Continuants	33
3.7	Three-dimensional frieze relation	35
3.7.1	Definition of λ -lengths	36
3.7.2	Ptolemy relation	36
3.7.3	Frieze pattern in higher dimensions	38
4	Suggestions for further work	39

1 Introduction

This paper is dedicated to the study of multidimensional continued fractions for subtractive algorithms based on integer invariants of their *sails*. (Sails are polyhedral surfaces associated to continued fractions.) We introduce *Farey polyhedra*, generalisations of Klein polyhedra in two dimensions, and study their properties and combinatorics. Finally we define a notion of higher dimensional frieze patterns, analogous to Conway-Coxeter frieze patterns.

This section is organised as follows. We start with a brief introduction to the subject areas in Subsection 1.1. We discuss our main contributions and provide an overview of the organisation of the paper in Subsection 1.2.

1.1 History and background

Multidimensional continued fractions. The question on generalisation of continued fractions to the multidimensional case was raised for the first time in 1868 by C. G. J. Jacobi (see [20]).

One of the first generalisations of continued fractions was proposed by F. Klein [29, 30] in 1895. F. Klein considered the cones in three-dimensional space; he introduced polyhedral surfaces that are now called *sails* (the boundaries of the convex hulls of all integer points inside the cone). Nearly 30 years ago V. I. Arnold initiated a detailed study of the geometric and combinatoric structures of Klein's polyhedra (see e.g. in [1, 2]). His suggestion was to examine the geometry and combinatorics of continued fractions via integer lattice invariants such as integer congruence classes of the faces of the sails, their quantities and frequencies, integer angles between the faces, integer distances, volumes, and so on.

H. Tsuchihashi [49] found the connection between periodic multidimensional continued fractions and multidimensional cusp singularities. J.-O. Moussafer in [41] and O. German in [15] studied the relationship between the sails of multidimensional continued fractions and Hilbert bases. Statistical properties of sails were studied by M. L. Kontsevich and Yu. M. Suhov in [31]. Multidimensional continued fractions appear in rigidity theory [27] and toric geometry [38]. Some examples of the periodic multidimensional sails were calculated in the papers [32, 33] by E. Korikina, [35] by G. Lachaud, [10, 43] by A. D. Bruno and V. I. Parusnikov, and the first author [25, 26] (see also [8, 22]). For the classical theory of regular continued fractions we refer to [28].

Another famous generalisation of continued fractions was proposed in [44, 45] by O. Perron in 1907. O. Perron invented an algorithm that produces approximations of a fixed direction (similarly to the continued fraction algorithm). Later his algorithm was referred to as the *Jacobi-Perron algorithm*. The Jacobi-Perron algorithm was further modified to numerous *subtractive algorithms*. Here we would like to mention the ordered Jacobi-Perron algorithm (OJPA) [18, 46], Brun's algorithm [6, 9], and the fully subtractive algorithm by F. Schweiger [47].

Technically speaking, Klein's approach to Jacobi's question works with cones rather than with a single direction, distinct from all subtractive algorithms. For this reason there is no straightforward matching between their properties. It is worth mentioning that in the classical two-dimensional case both Klein's and Perron's theories provide the same continued fractions.

Hermite's problem. For the last 100 years subtractive algorithms and Klein's polyhedra were competing techniques to approach various mathematical problems. Let us consider one of such problems. *Hermite's problem* of 1848 asks to find a comprehensive description of cubic irrationalities (i.e. the roots of cubic irreducible polynomials over \mathbb{Q} with integer coefficients) in terms of some eventually periodic sequences. The answer to this question would generalise Lagrange's theorem on the periodicity of regular continued fractions for quadratic irrationalities.

Klein polyhedra are doubly-periodic for triples of conjugate vectors, however the constructive combinatorial description of such periods is not yet known. V. I. Arnold formulated several famous open problems on the quotient tori decompositions of fundamental domains that lead to the generalisation of the Lagrange's theorem on classical periodicity to the multidimensional case (see, e.g., in [22]). Partial results in this directions were obtained in papers [16, 35].

Contrary to the situation for Klein polyhedra, the description of periods for subtractive algorithms is simple, as it is conjectured that most of the subtractive algorithms are not necessarily periodic for cubic vectors. (For further discussions see, e.g. Jacobi's last theorem for the Jacobi-Perron algorithm in Section 27.4 of [22].) It is only recently that the first periodic subtractive algorithms were constructed [23, 24]. It is remarkable that the periodicity proof of the \sin^2 -algorithm of [23] (the only subtractive algorithm which is proven to be periodic for cubic irrationalities) substantially involves the periodicity of Klein polyhedra.

Geometry of subtractive algorithms. The first steps in studying the geometry of subtractive algorithms were done in 2001 when T. Garrity introduced triangle sequences [14]. Together with

his coauthors he proved several dynamical results and a criterion on convergence in [3]. In another paper [5] he studied the Farey partition and generalises the Minkovskii φ -function for it. Later in 2008 G. Panti considered another triangle map in [42].

We aim to develop new techniques of Klein polyhedra adjusted to subtractive algorithms. We pick one particular subtractive algorithm that suits our purposes the best: *the Farey summation algorithm*, corresponding to the Farey partition introduced [5]. This algorithm is based on the most straightforward generalisation of Farey summation to the higher dimensional cases.

This algorithm has remarkable properties. It admits a natural generalisation of the nose stretching algorithm (see [1] for the classical nose stretching algorithm) and a remarkable convergence set (studied in detail in [34]). Note that the dual to the Farey summation algorithm is the Meester algorithm introduced in 1989 by R. W. J Meester in [36]. Namely the Meester algorithm acts as the Gauss map for the Farey summation algorithm. As follows from the main theorem of [34] (on Meester algorithm), the infinite sequences of cones produced by the Farey summation algorithm do not converge to a single ray almost everywhere. As one of the consequences we get that Jacobi's last theorem does not hold for the Farey summation algorithm (there are cubic irrationalities with non-periodic continued fractions).

Informally speaking the Farey summation algorithm is the simplest algorithm from the geometric perspective. This is partially due to its rigid version of nose stretching algorithm, see Subsection 2.5.2 below. Note that the proposed geometric techniques can be generalised for other subtractive algorithms. All but a few of the properties will have straightforward generalisations.

Frieze patterns and triangulated polygons. In the classical two-dimensional case *frieze patterns* are tables of numbers introduced by H. Coxeter [13] and studied together with J. Conway in [12]. In the latter paper a correspondence between frieze patterns and triangulations of convex polygons was found, which in turn has provided a connection with the more recent study of cluster algebras (see, e.g. in [4, 39]).

The correspondence may be understood in the following two ways. First, counting the number of triangles incident to each vertex in a triangulation provides a sequence that uniquely defines the frieze pattern up to cyclic permutations of the elements in the sequence. Second, by embedding the polygon triangulation to the Farey complex in the hyperbolic plane, one associates rational numbers to the vertices of the original polygon. There exists an elegant formula connecting rational numbers at pairs of vertices to each element of the frieze pattern corresponding to the triangulation, see the paper [48] by I. Short for more details. Frieze patterns can be thought of as encoding the combinatorics of triangulated polygons.

In this paper we introduce prismatic diagrams that serve as an important combinatorial invariant of Farey polyhedra. We use the combinatorics of prismatic diagrams to define three-dimensional frieze patterns where each element is associated to a pair of vertices on the prismatic diagram. Similar to the two-dimensional case, three-dimensional frieze patterns admit a version of the Ptolemy relation for pairs of faces in a prismatic diagram.

1.2 Main results

In this paper we generalise Klein polyhedra and their sails to higher dimensional cases and study their properties. In particular we introduce frieze patterns in higher dimensions.

Definition of Farey polyhedra. Our generalisation of Klein polyhedra is provided by the following four basic algorithmic definitions:

- **Algorithm 2.8:** first we generate a tessellation of \mathbb{Z}^2 that is equivalent to the tessellation of the hyperbolic plane by the Farey graph;

- **Algorithm 2.18:** for a ray emanating from the origin we consider the union of simplices intersecting the ray. This is the *Farey polyhedron*, the central object of study, and was first studied by T. Garrity in [14];
- **Algorithm 2.32:** the Meester algorithm, introduced by R. W. J Meester in [36], is the subtractive algorithm that defines continued fractions for the Farey polyhedron;
- **Algorithm 2.42:** finally the *nose stretching algorithm* provides a reconstruction of the Farey polyhedron from the continued fraction.

Combinatorics of Farey polyhedra, prismatic diagrams, and sails. We introduce a combinatorial description of the boundaries of Farey polyhedra using *prismatic diagrams*, special polytopes with fixed triangulations. Prismatic diagrams are complete invariants of Farey polyhedra (see Theorem 3.27). They generalise the combinatorial description of triangulated polygons given by Farey boats, introduced by S. Morier-Genoud and V. Ovsienko in [40]. Prismatic diagrams allow us to generalise several important notions of the geometry of continued fractions to the multidimensional case: sails and LLS sequences, whose elements encode the elements of the Farey summation continued fractions (see Definition 3.40 and Theorem 3.57). Prismatic diagrams and their LLS-sequences are suitable tools with which to study geometric aspects of the Farey summation algorithm.

Generalised frieze patterns. In 1973 J. Conway and H. S. M. Coxeter discovered a one-to-one correspondence between triangulated polygons and frieze patterns, where each pair of vertices corresponds to a unique frieze element. The defining relation of frieze patterns is then interpreted as a Ptolemy relation on the edges of the corresponding triangulated polygon.

A natural question to ask is as follows: *is there an analogous frieze-like Ptolemy relation for faces of the Farey polyhedron, described by invariants of the prismatic diagram?* We answer this question in the affirmative in Theorem 3.80. We use newly defined three-dimensional continuants to find λ -lengths, values assigned to pairs of vertices of Farey polyhedra. We show that the 3×3 matrix of λ -lengths defined by pairs of faces of the Farey polyhedron have determinant 1.

Organisation of the paper. We start in Section 2 with the discussion of Farey tessellation and the construction of the *Farey polyhedra*, the central objects of study in this paper.

We recall some basic notions of integer geometry in Subsection 2.1 before defining the Farey tessellation in the integer setting in Subsection 2.2. Farey polyhedra are defined by the Farey summation algorithm, described in Subsection 2.3. Here we also introduce important terminology used throughout the paper. A multidimensional continued fraction is then defined from the Farey summation algorithm in Subsection 2.4.

In Subsection 2.5 we recall the algorithm of R. W. J Meester and note its equivalence to the continued fraction defined by the Farey summation algorithm. Finally we recall the situation of convergence of the Meester algorithm in Subsection 2.6, and relate these known results to the Farey summation algorithm.

In Section 3 we study the properties of Farey polyhedra. We introduce important invariants of the polyhedra, including the combinatoric prismatic diagrams.

We start with Subsection 3.1 in which we discuss the basic properties of the Farey tessellation. Prismatic diagrams are defined in Subsection 3.2.

We define generalisations of the important integer invariants, sails and LLS-sequences, from prismatic diagrams in Subsection 3.3.

We study the matrix decomposition of the Farey summation algorithm in Subsection 3.4. This is a prerequisite for the study of LLS sequences in Subsection 3.5. The matrix decomposition admits a natural generalisation of the notion of *continuants*. We discuss this in Subsection 3.6.

In Subsection 3.5 we describe the Ptolemy relation for Farey polyhedra, and introduce three-dimensional frieze patterns.

Finally in Section 4 we mention some open questions in the area.

2 Farey tessellation and related algorithms

We start this section with a short discussion on integer geometry, which forms the basis of much of the paper, followed by a description of the Farey tessellation. Then we define the Farey summation and the Meester algorithms which are closely linked together, and they are both related to the geometric continued fraction that we study. We close the section with some short words on the convergence of these algorithms.

2.1 A few words on integer geometry

Let us fix some integer $n \geq 2$. A point is said to be *integer* if its coordinates are integer. All integer points form the lattice of integer points \mathbb{Z}^n . A vector, segment, polygon, or polytope are *integer* if all their vertices are integer.

We say that an affine transformation is *integer* if it preserves the lattice of integer points. The set of affine transformation is denoted by $\text{Aff}(n, \mathbb{Z})$. Any integer affine transformation is a composition of a $\text{GL}(n, \mathbb{Z})$ matrix multiplication and a shift on an integer vector.

Definition 2.1. Two sets S_1 and S_2 are *integer congruent* if there is an integer affine transformation providing a bijection between S_1 and S_2 .

Definition 2.2. *Integer length* of an integer segment is the number of integer points in the interior of this segment plus one. The *integer distance* between two integer points is the integer length of the segment connecting them.

Definition 2.3. Integer volume of a tetrahedron generated by linear independent integer vectors $V = (v_i)_{i=1}^k$ is the index of the sublattice generated by V in integer lattice of the plane spanning V . Denote it by $\text{IV}(V)$.

In order to avoid repeating the fact that our coordinates are relatively prime, we introduce the notion of a unit integer circle.

Definition 2.4. The *unit integer sphere* $\mathbb{Z}S^{n-1} \subset \mathbb{Z}^n$ *centred at the origin* is the set of all points whose integer distance to the origin equals 1.

2.2 Farey tessellation in higher dimensions

Let us describe the Farey tessellation, recalling first the familiar two-dimensional case.

2.2.1 Construction of the Farey tessellation

Consider two rational numbers p/q and r/s defined by the two pairs of relatively prime numbers (p, q) and (r, s) . The *Farey sum* of these two numbers is defined as follows:

$$\frac{p}{q} \oplus \frac{r}{s} = \frac{p+r}{q+s}.$$

Let us first projectivise this summation (this will enable us to have $\infty = (1 : 0)$):

$$(p : q) \oplus (r : s) = (p + q : r + s).$$

In lattice geometry there is a natural selection of $(p : q)$ for a projective point (up to the choice of the sum). Namely we associate a projective point $(p : q)$ to a collinear point on the integer unit circle $\mathbb{Z}S^1$. In most of the paper we work with non-negative coordinates, so the point of $\mathbb{Z}S^1$ is actually uniquely defined. For non-negative rational pairs of the unit circle we have the *Farey summation* as well:

$$(p, q) \oplus (r, s) = (p + q, r + s).$$

It is interesting to note that such Farey summation in $\mathbb{Z}S^{n-1}$ simply coincides with the integer vector summation.

Let us generalise Farey addition to the multi-dimensional case as a vector addition; its projection to the plane $x_n = 1$ or alternatively to the plane $x_1 + \dots + x_n = 1$ will be different versions of rational Farey additions (see, e.g. in [5]).

Definition 2.5. Let $U_1(u_1, \dots, u_n)$ and $V_2(v_1, \dots, v_n)$ be two arbitrary points in \mathbb{Z}^n . Then their *Farey sum* is defined as

$$A_1 \oplus A_2 = (u_1 + v_1, \dots, u_n + v_n).$$

Now we are ready to give the major building block of the multidimensional Farey tessellation that we describe later in Algorithm 2.8.

Definition 2.6. Let $V_1 \dots V_k$ be a simplex in $\mathbb{Z}S^n$. We say that its *Farey pyramid* is the simplex $WV_1 \dots V_k$, where $W = V_1 \oplus \dots \oplus V_k$, $k \leq n$. Here W is the vertex of the pyramid and $V_1 \dots V_k$ is its base.

We say that a face of the Farey pyramid is *side/base* if it contains/does not contain W .

In the degenerate case $k = 1$ the vertex W coincides with the base V_1 . In this case we say that such pyramid does not have side faces.

Remark 2.7. Side faces of the Farey pyramid can have any dimension from 0 to $k - 1$.

Technically we do not require W to be in $\mathbb{Z}S^{n-1}$, however in the below construction it will be always the case.

Algorithm 2.8 (Farey tessellation). Consider the non-negative orthant, and let OE_i be its coordinate vectors for $i = 1, \dots, n$.

Base of construction: Consider the set S of all faces (of all possible dimensions) of the $(n - 1)$ -dimensional tetrahedron $E_1 \dots E_n$.

Step of construction: Let S be the set of faces from the previous step. At this step for every face in S we add all side faces of its Farey pyramid.

We iterate the step of construction finite or infinitely many times.

- the Farey pyramids of the resulting set S are said to be *Farey tessellation simplices*;
- the decomposition of the positive orthant into Farey tessellation simplices tetrahedra is said to be *Farey tessellation* of the positive orthant. (For completeness, we add the basis tetrahedron to the tessellation.)

Remark 2.9. The central projection of all edges of the Farey tessellation to the plane $x_n = 1$, namely

$$(x_1, \dots, x_n) \rightarrow \left(\frac{x_1}{x_n}, \dots, \frac{x_{n-1}}{x_n} \right),$$

provides a triangulation of the basis simplex given by *triangle sequences* of [5]. This triangulation is known as the *Farey partition* of the simplex.

Let us mention the following quantitative properties of the Farey tessellation.

Proposition 2.10. *The following holds:*

- *The integer volume of a Farey simplex of dimension k equals $k-1$ (with the only exception for the basis one with integer volume equals 1);*
- *The pyramid with the vertex at the origin and the base in a face of any Farey simplex has a unit integer volume.*

Proof. Consider a Farey tessellation simplex $V_1 \dots V_k$. Both statements follow from the fact that in the integer basis of the vertices of the coordinates OV_1, \dots, OV_k , the new added point $W = AV_1 \oplus \dots \oplus V_k = (1, \dots, 1, 0, \dots, 0)$ (here the first k coordinates equal 1). Hence all the Farey tetrahedra are integer congruent and have the integer volume equals $k-1$; and the pyramids for all the faces of the tetrahedron are of unit volume. \square

2.2.2 Farey and quasi-Farey nets

Recall the following general definition.

Definition 2.11. We say that an integer tetrahedron of dimension n in \mathbb{Z}^n is *unimodular* if the vectors of its edges generate the lattice \mathbb{Z}^n .

Consider a tessellation T of the positive orthant. Let us centrally project it to the coordinate triangle of the plane $x_n = 1$. The image of the edges of the tessellation is called the *net* of this tessellation.

Definition 2.12. A net is said to be *Farey* if all the tetrahedra in the original tessellation are unimodular.

Note that Farey nets were introduced by A. Hurwitz in [19] and further developed by D.J. Grabner in [17].

In what follows we consider a slightly extended notion of Farey nets.

We say that a convex polytope with integer vertices is *empty* if it does not contain integer points distinct to its vertices (both in the interior and at the boundary).

Definition 2.13. A net is said to be *quasi-Farey* if all the tetrahedra in the original tessellation are empty.

Remark 2.14. In the two-dimensional case all empty triangles are integer congruent to the coordinate one. However in higher dimensions there are infinitely many different types of empty tetrahedra that are integer non-congruent to each other. All empty tetrahedra of dimension three have been classified by G.K. White in [51]. The complete description of empty tetrahedra in dimension greater than 3 is not known.

Proposition 2.15. *The Farey tessellation of the coordinate cone generates a quasi-Farey net.*

Proof. Consider any Farey tetrahedron T . By Proposition 2.10, the volumes of the pyramids with centre at the origin and bases at faces of T equal 1. Therefore, they are all empty, and hence T is empty as well. \square

Remark 2.16. The quasi-Farey net of the Farey summation algorithm was studied by O.R. Beaver and T. Garrity in [5] in dimension 3. The corresponding continued fraction map on the net is called *the Triangle map*.

Remark 2.17. Later in Proposition 3.1 we show that the closure of the union of all the Farey simplices is the whole non-negative orthant and that two Farey tetrahedra do not intersect.

2.3 Description of the Farey summation algorithm

Let us describe a natural continued fraction algorithm generated by the Farey tessellation.

Algorithm 2.18 (Farey summation algorithm). The *Farey summation algorithm* is the algorithm that produces a (finite or infinite) sequence of simplices T_i for a given vector $v \in \mathbb{R}_+^n$.

Base of the algorithm: Let S_0 be the basis simplex $OE_1 \dots E_n$. We formally set the simplex $E_1 \dots E_n$ to be the *deck* (zero yard) T_0 of the algorithm. Here a *yard* is an $n - 1$ dimension simplex through which v passes.

Step i of the algorithm: In the previous step we have constructed the $(i-1)$ -th yard T_{i-1} . Denote by S_i the Farey pyramid with base T_{i-1} , we call it the *i -th Farey pyramid* of the Farey summation algorithm. Let us show how to construct the *i -th yard* T_i . Note that the ray in the direction of v intersects exactly one side face of S_i of any dimension in its interior (here interiors of zero-dimensional faces is the vertex itself). We set T_i to be this face.

Termination of the algorithm: In case the next chosen simplex is a single vertex, the algorithm naturally terminates. Otherwise, the algorithm produces the infinite sequence of yards.

The last yard is called *the (crow's) nest*; the last vertex is called the *pennant*.

Definition 2.19. The union of the Farey pyramids formed by the algorithm is called the *Farey polyhedron*.

Note that we have natural induced notions of the *deck*, the *nest*, the *pennant*, and the *yards* for the Farey polyhedron.

Definition 2.20. We say that the i -th yard ($i \geq 1$) of a Farey polyhedron is *principal* if either the dimension drops at Step $i+1$ or if the index of the basis vector that we change at Step $i+1$ is different to the index of the basis vector at Step i . The deck and the nest are considered to be *principal* by default.

Let us formulate the following important properties of Farey pyramids.

Proposition 2.21. *Two consecutive principal yards of a Farey polyhedron share a face of codimension 1 (with respect to the yard).*

The convex hull of two consecutive principal yards is a simplex; it coincides with the union of the Farey pyramids between them. \square

As we will see later, while defining continued fractions we group consecutive Farey pyramids of the Farey summation algorithm together as follows.

Definition 2.22. The convex hull of two consecutive principal yards is said to be a *division simplex* for the Farey polyhedron (division tetrahedron in three-dimension).

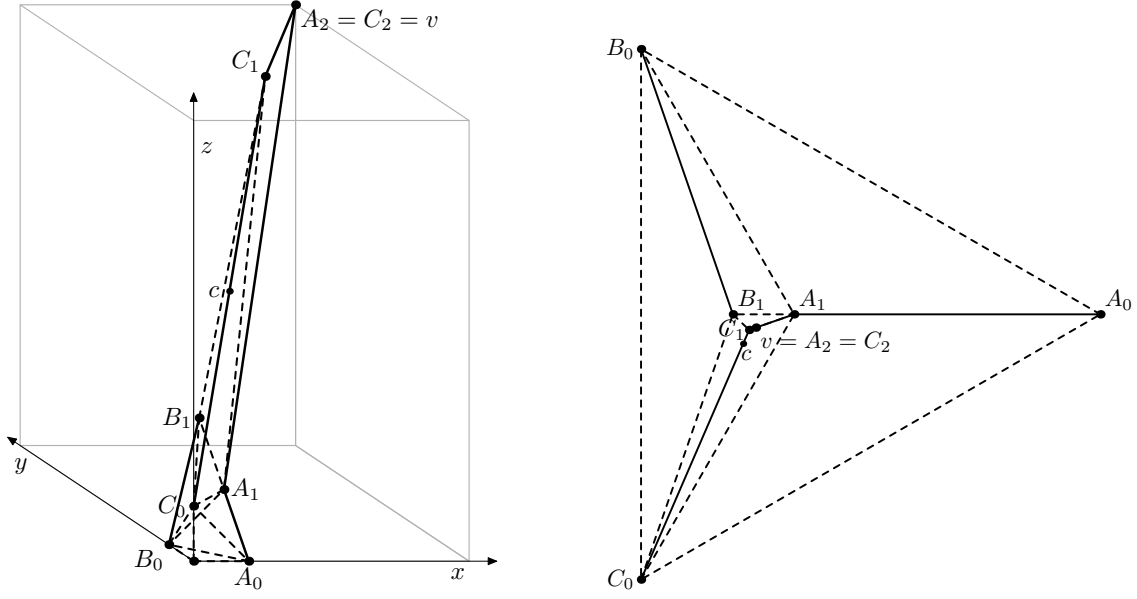


Figure 1: Farey summation algorithm for $(5, 7, 8)$ (left) and its central projection to the plane $x + y + z = 1$.

Remark 2.23. Let T_k and T_l ($k < l$) be two yards for some vector v . Then the dimension of T_l does not exceed the dimension of T_k . (The same for S_k and S_l .)

Remark 2.24. Historically a multidimensional continued fraction algorithm is called *Farey* if its net is Farey. However, while the multidimensional Farey tessellation of the Farey summation algorithm provides the most straightforward generalisation of the Farey tessellation of the plane, its corresponding projection is a quasi-Farey net (and not a Farey may). For this reason the Farey summation algorithm is not really a Farey algorithm (however it provides the direct generalisation of the Farey addition).

Remark 2.25. The nautical terminology is motivated by two previous unrelated definitions: the *sails* first studied by F. Klein and so named by V. I. Arnold, and *Farey boats* introduced by S. Morier-Genoud and V. Ovsienko, which we study further in Subsection 3.2.

Example 2.26. In Figure 1 we show the Farey summation algorithm for the vector $(5, 7, 8)$.

- *Base:* We start with the basis tetrahedron $S_0 = OA_0B_0C_0$ and set $T_0 = A_0B_0C_0$.
- *Step 1:* We construct the Farey pyramid $S_1 = A_0B_0C_0A_1$ with $A_1 = A_0 \oplus B_0 \oplus C_0 = (1, 1, 1)$. The vector v intersects the side $A_1B_0C_0$ (seen clearly from the right picture). Hence $T_1 = A_1B_0C_0$.
- *Step 2:* The next Farey pyramid is $A_1B_0C_0B_1$ with $B_1 = A_1 \oplus B_0 \oplus C_0 = (1, 2, 2)$. Hence $T_2 = A_1B_1C_0$.
- *Step 3:* $S_3 = A_1B_1C_0c$ with $c = (2, 3, 4)$; $T_3 = A_1B_1c$.

- *Step 4:* $S_4 = A_1 B_1 c C_1$ with $C_1 = (4, 6, 7)$;
 $T_4 = A_1 C_1$. Note that here the yard is one-dimensional.
- *Step 5:* $S_5 = A_1 C_1 v$. Since T_4 is one-dimensional, S_5 is two-dimensional. Here we arrive to the final vector $v = A_1 \oplus C_1 = (5, 7, 8)$.
The algorithm terminates here.

In our notation all the yards T_i except for $i = 3$ are principal; T_0 is a deck; T_4 is a nest; and the last vector v is a pennant.

In Figure 1 (Left) we show all the Farey simplices for $(5, 7, 8)$ in the space; in Figure 1 (Right) we show the central projection all the Farey simplices to the plane $x + y + z = 1$. As we will see later the point v can be labeled either as A_2 or C_2 .

2.4 Definition of Farey summation continued fractions

We describe an algorithm for *Farey summation continued fractions*, based on the Farey summation algorithm. For simplicity we work essentially in the three-dimensional case.

2.4.1 Enumeration of vertices

Let us first enumerate all the vertices in all side triangles used in the algorithm. Our base external triangle is $V_{0,1} = (1, 0, 0)$, $V_{0,2} = (0, 1, 0)$, $V_{0,3} = (0, 0, 1)$.

Assume that the vertices for the external simplex in Step i are already enumerated, say $V_{i,1}$, $V_{i,2}$, and $V_{i,3}$. Let us enumerate the vertices of the external simplex in Step $i+1$ in the following way: in this step there is only one vertex that is replaced by a new one; set the index of the new vertex to be the same as the replaced vertex (while the indices of the unchanged vectors stay the same). For instance, if $V_{i,2}$ is replaced then we label $V_{i+1,1} = V_{i,1}$; $V_{i+1,2} = V_{i,1} + V_{i,2} + V_{i,3}$; $V_{i+1,3} = V_{i,3}$.

2.4.2 Tabulation of the algorithm

In the three-dimensional case the algorithm splits into two stages.

Stage 1. Step i is in this stage if the i -th yard is two-dimensional. Define $r_i \in \{1, 2, 3\}$ to be the index of the vertex that is changing.

Let us write the sequence of r_i generated in this stage in the following form:

$$1^{a_1} 2^{a_2} 3^{a_3} 1^{a_4} \dots,$$

where a_j are the multiplicities of the consequent indices. Note that some a_i may be zero, however we require no two zeroes in a row except when passing to Stage 2 (a_{k-1} and a_k), and at the beginning (a_1 and a_2).

Stage 2. Step $k+i$ is in this stage the $k+i$ -th yard is one-dimensional. Here we change only the vertices with indices $s, t \in \{1, 2, 3\}$ such that $s \equiv k$ and $t \equiv k+1$ modulo 3.

Again we can abbreviate the sequence of changed indices as:

$$s^{b_1} t^{b_2} s^{b_3} t^{b_4} \dots$$

(note that a_k , a_{k-1} , and b_1 may necessarily be zeroes while passing from Stage 1 to Stage 2).

Remark 2.27. The proposed tabulation is very similar to LR-notation in the Farey graphs (see e.g. in [22] for more details).

Finally we join both of the sequences (a_i) and (b_j) together to form a single sequence.

Definition 2.28. Consider a vector v with positive coordinates. Let it generate the sequences (a_i) and (b_j) described above. The sequence

$$[a_1; a_2 : \dots : a_k | b_1 : \dots : b_l]$$

is said to be the *Farey summation continued fraction* for a vector v . In case the sequences (a_i) or (b_i) are infinite we write

$$[a_1; a_2 : \dots |] \quad \text{and} \quad [a_1; a_2 : \dots : a_k | b_1 : \dots]$$

respectively.

Remark 2.29. By construction all finite and infinite sequences (a_i) and (b_j) of non-negative elements are realised as Farey summation continued fractions for some vector v with the following list of exceptions:

- There are no two consecutive zeroes in (a_i) except for:
 - $a_1 = a_2 = 0$ and $a_3 \neq 0$;
 - $a_{k-1} = a_k = 0$, $a_{k-2} \neq 0$, and (b_j) contains at least one positive element;
- If (b_j) is empty, then $a_k \neq 0$.
- All b_i are positive with the only exception that b_1 can be 0 in the case $l \geq 2$.

Example 2.30. Consider a vector $v = (5, 7, 8)$. In Example 2.26 we have discussed the Farey summation algorithm for v . Now we can write the Farey summation continued fraction for it:

$$[1; 1 : 2 : 0 : 0 | 1].$$

Note that we add two zeroes since our pair $(s=3, t=1)$ follows after $(s=1, t=2)$ and $(s=2, t=3)$ that we skip.

Note also that the sum of all elements is 5, which is equal to the number of steps (Farey pyramids) in the Farey summation algorithm.

2.5 Meester algorithm

Our next goal is to describe the Meester algorithm which is a Jacobi-Peron type subtractive algorithm. Meester algorithm plays the same role for the Farey summation continued fractions as the Euclidean algorithm plays for the continued fractions algorithm. In this subsection we work in an arbitrary dimension.

2.5.1 A general definition

Let us begin with a small remark.

Remark 2.31. In the Meester algorithm below we fix the order of basis vectors. A different ordering of basis vectors will lead to slightly different continued fractions but the same tessellation.

Algorithm 2.32 (Meester algorithm). We start with an n -tuple of non-negative real numbers (v_1, \dots, v_n) . While there are no zero coordinates we perform the following iteration steps.

The i -th iteration step is as follows ($i = 1, \dots$):

- Let $j \in \{1, \dots, n\}$ satisfy $j = i \bmod n$.
- If the j -th coordinate is zero then we go straight to the next step. Otherwise we subtract the j -th coordinate from all other non-zero coordinates simultaneously as many times as it is possible for all to remain non-negative: denote the number of times we have subtracted by a_i (note that $a_i = 0$ is possible). Denote also the resulting vector as $(v_{1,i}, \dots, v_{n,i})$.
- As a result of the previous item we obtain a new n -tuple of non-negative real numbers. We keep the number a_i as the element of the continued fraction.

The algorithm terminates if we have a single non-zero coordinate.

For any $j \in 1, \dots, n$ consider the sequence of a single coordinate $(v_{j,i})$. Denote by s_j the integer for which $v_{j,s_j} = 0$ and $v_{j,s_j-1} > 0$. If the sequence $v_{j,i}$ is always positive, then we do not assign any value for s_j .

Note: We introduce s_j to keep track of the step at which the j -coordinate becomes 0. This is used later when reconstructing the Farey polyhedron from the continued fraction.

As the output of Meester algorithm we have two items:

- a sequence of non-negative integers (a_i) ;
- a sequence of $(s_{j_1}, \dots, s_{j_k})$ enumerated in the increasing order. Here the number k denotes the number of s_j for which the values are assigned during the algorithm execution (here $k \leq n - 1$).

Finally we write the elements a_i in the form of continued fraction.

First, let us assume that the algorithm is finite. Then for the sequence $(s_{j_t})_{t=1}^k$ we have $k = n - 1$, as after step N we have $n - 1$ zero coordinates. We also do not indicate the last $s_{j_{n-1}}$ as this denotes a change occurring at the terminal step of the algorithm. The following expression is called the *Meester algorithm continued fraction*:

$$[a_1; \dots : a_{s_{j_1}} \mid_{j_1} a_{s_{j_1}+1} : \dots : a_{s_{j_2}} \mid_{j_2} a_{s_{j_2}+1} : \dots : a_{s_{j_{n-2}}} \mid_{j_{n-2}} a_{s_{j_{n-2}+1}} : \dots : a_N].$$

In case the algorithm does not terminate, k could be any number of $\{1, \dots, n - 2\}$. The corresponding continued fraction is infinite:

$$[a_1; \dots : a_{s_{j_1}} \mid_{j_1} a_{s_{j_1}+1} : \dots : a_{s_{j_2}} \mid_{j_2} a_{s_{j_2}+1} : \dots : a_{s_{j_k}} \mid_{j_k} a_{s_{j_k}+1} : a_{s_{j_k}+2} : \dots].$$

For both finite and infinite continued fractions: after the symbol \mid_{j_s} is used we do not include a_i , where $i = j_s \bmod n$, in the continued fraction, since the values of a_i are not assigned at these steps.

Remark 2.33. The Meester algorithm has been previously introduced and studied in [34, 36, 37].

Example 2.34. Consider the example of $(55, 10, 67)$. The Meester algorithm produces

$$(55, 10, 67) \xrightarrow{0,5} (5, 10, 17) \xrightarrow{0,2} (5, \underline{0}, 7) \xrightarrow{0,1} (5, 0, 2) \xrightarrow{2} (1, 0, 2) \xrightarrow{2} (1, 0, \underline{0}).$$

The zeroes denote steps where no subtraction is possible. The sequence of a_i here is $(0, 5, 0, 2, 0, 1, 2, 2)$. Further we have:

- $s_{j_1} = 4$ and $j_1 = 2$, from the third vector we have the zero second coordinate (underlined);

- $s_{j_2} = 8$ and $j_2 = 3$ in the last vector the third coordinate is zero (underlined). For simplicity we do not show $s_{j_2} = 8$ in the continued fraction, which stands in the last position (after which no steps are done).

Therefore, the Farey summation continued fraction for $(55, 10, 67)$ is as follows:

$$[0; 5 : 0 : 2(a_{s_{j_1}=4}) |_{j_1=2} 0 : 1 : 2 : 2].$$

Remark 2.35. On the i -th step we get the sequence (a_1, \dots, a_i) and the vector $V_i = (v_{1,i}, \dots, v_{n,i})$. A basis W_i generated by the Farey summation continued fraction $[a_1; \dots : a_i]$ gives us the i -th *convergent*, while V_i is the *remainder*. In fact the remainder V_i is generated by

$$[0; \dots : 0 |_{j_1} \dots 0 |_{j_k} \dots 0 : a_{i+1} : \dots : a_N].$$

Here the number of initial zeroes coincides with the index on the Step $i+1$; since the j_1, \dots, j_k are all the indices removed before Step $i+1$.

Example 2.36. For the point $(55, 10, 67)$ with continued fraction $[0; 5 : 0 : 2 |_2 : 0 : 1 : 2 : 2]$, the remainder when $i = 6$ is $V_6 = (5, 0, 2) = [0^4; |_2 0^2 : 2 : 2] = [0; |_2 2 : 2]$.

Remark 2.37. Note that the value of the non-zero coordinate in the final step of the algorithm is the greatest common divisor of the initial coordinates, just as in the classical Euclidean algorithm.

The following proposition links the geometrical nature of Farey summation algorithm and the number theoretical nature of Meester-algorithm.

Proposition 2.38. *Let v be a non-zero point of the positive orthant. Then the Meester algorithm for v generates the same continued fraction as the Farey summation algorithm.*

The only difference in writing is as follows. One should replace

$$|_j \mapsto 0 : \dots : 0 : |,$$

where the number of zeroes, it is the number of cyclic transpositions to exclude the correct coordinate. In the three-dimensional case it is either 0, 1, or 2. \square

Example 2.39. For the sequence of Example 2.30 we have

$$(5, 7, 8) \rightarrow (5, 2, 3) \rightarrow (3, 2, 1) \rightarrow (1, 0, 1) \rightarrow (1, 0, 0).$$

The corresponding Meester algorithm continued fractions is

$$[1; 1 : 2 |_2 1] = [1; 1 : 2 : 0 : 0 | 1].$$

2.5.2 Extended Meester algorithm continued fraction

Recall that for ordinary continued fractions we have the following obvious relation:

$$[a_0; \dots : a_n] = [a_0; \dots : a_n - 1 : 1]$$

(here we assume that $a_n > 1$). Note that the Euclidean algorithm does not generate $[a_0; \dots : a_n - 1 : 1]$, however both forms find use in the literature. For example, in integer geometry one may be interested solely in odd length continued fractions. We consider analogous equivalent continued fractions for the Farey summation algorithm.

Definition 2.40. Consider the Meester algorithm continued fraction. Let the Farey addition at the last step be on k points. Let us replace the last element a_n of the continued fraction by a sequence $(a_{n-1}, 0, \dots, 0, 1)$, where the number of zeroes does not exceed $k - 2$. We say that the obtained sequence is the *extended Meester algorithm continued fraction*.

Example 2.41. For $(5, 7, 8)$ we have the following two extended Meester algorithm continued fractions

$$[1; 1 : 2 |_2 1] = [1; 1 : 2 |_2 0 : 1].$$

2.5.3 Reconstruction of Farey simplices for a given continued fraction

Let us show how to reconstruct all the Farey simplices that were used in the Farey summation algorithm from the Farey summation continued fraction.

Algorithm 2.42 (Nose stretching algorithm). We start with an n -tuple of integer basis vectors (E_1, \dots, E_n) . We are also given a Farey summation continued fraction

$$\alpha = [a_1; \dots : a_{s_{j_1}} |_{j_1} a_{s_{j_1}+1} : \dots : a_{s_{j_2}} |_{j_2} a_{s_{j_2}+1} : \dots : a_{s_{j_{n-2}}} |_{j_{n-2}} a_{s_{j_{n-2}+1}} : \dots : a_N].$$

Step of the algorithm. On Step s we get several ordered vectors (V_1, \dots, V_n) . The step contains two stages.

Generating vectors for the next step: We start this step with the vector V_j , the first non-zero vector to the right of $V_s \bmod n$. In other words, we skip any zero vectors. Let k be the number of symbols $|_i$ occurring in all previous steps. We denote

$$\hat{V} = V_j \oplus a_s(V_1 \oplus \dots \oplus V_{j-1} \oplus V_{j+1} \oplus \dots \oplus V_n)$$

We relabel $V_j = \hat{V}$, and so the data for the next step will be the vectors

$$V_1, \dots, V_n.$$

Vector erasing: The vectors V_i whose indices are given by symbols $|_i$ occurring on Step s are all replaced with zero vectors.

Returning a Farey simplex T_s : On this step we return the Farey simplex

$$T_s = \text{conv}(V_1, \dots, V_n).$$

If the Farey summation continued fraction is finite then the algorithm is iterated until the last element, at which point all vectors except V_j are set to be the zero vector. The algorithm is iterated indefinitely otherwise. It generates the sequence of Farey simplices (T_s) that are used in the Farey summation algorithm for the vector v whose continued fraction is α .

Example 2.43. Let us study the case $v = (5, 7, 8)$ of Example 2.26, which has continued fraction $[1, 1, 2 |_2 1]$. We write the corresponding nose stretching algorithm for the basis vectors. For brevity we write the three vectors in the form of a 3×3 matrix.

$$\begin{pmatrix} 1 & 0 & 0 \\ 0 & 1 & 0 \\ 0 & 0 & 1 \end{pmatrix} \xrightarrow{1} \begin{pmatrix} 1 & 0 & 0 \\ 1 & 1 & 0 \\ 1 & 0 & 1 \end{pmatrix} \xrightarrow{1} \begin{pmatrix} 1 & 1 & 0 \\ 1 & 2 & 0 \\ 1 & 2 & 1 \end{pmatrix} \xrightarrow{2} \begin{pmatrix} 1 & 1 & 4 \\ 1 & 2 & 6 \\ 1 & 2 & 7 \end{pmatrix} \xrightarrow{|_2} \begin{pmatrix} 1 & 0 & 4 \\ 1 & 0 & 6 \\ 1 & 0 & 7 \end{pmatrix} \xrightarrow{1} \begin{pmatrix} 5 & 0 & 4 \\ 7 & 0 & 6 \\ 8 & 0 & 7 \end{pmatrix} \xrightarrow{(|_3)} \begin{pmatrix} 5 & 0 & 0 \\ 7 & 0 & 0 \\ 8 & 0 & 0 \end{pmatrix}$$

As output we have the only non zero vector, $v = (5, 7, 8)$. We omit the final $|_3$ in the continued fraction.

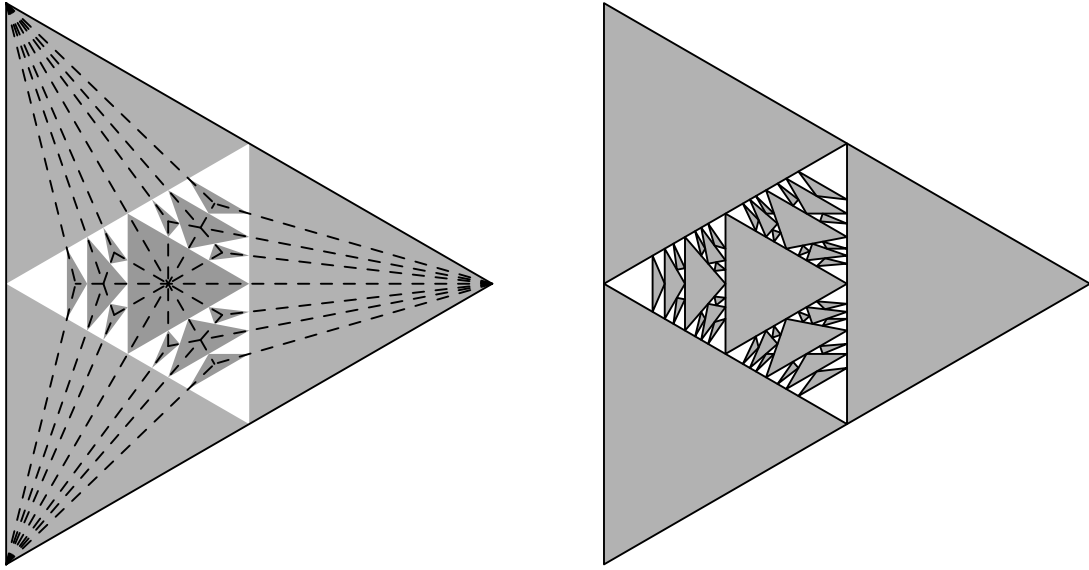


Figure 2: Meester algorithm divergence set (several iterations)

2.6 A few words on convergence of the Farey summation algorithm

Let us briefly discuss the convergence properties of the Farey summation algorithm. Without loss of generality we restrict to the three-dimensional case, the situation in the higher dimensional case is similar to \mathbb{R}^3 . The results of this section follow directly from [34].

2.6.1 The divergence set is everywhere dense

First of all note that the Farey tessellation converges to a single ray if and only if the Meester algorithm converges to $(0, 0, 0)$. It is interesting to observe that the Meester algorithm does not always converge to $(0, 0, 0)$ everywhere in the positive orthant (see [37] for the three-dimensional case; see [34] for the proof in the higher the dimensions).

As it was shown in [34] if at some iteration of the algorithm one of the coordinates exceeds the sum of the other two, then there is no convergence. For this reason the convergence set can be constructed by removing the “corner cones” generated by the vectors:

$$[a_1; \dots : a_n \mid 1], \quad [a_1; \dots : a_n : 0 \mid 1], \quad [a_1; \dots : a_n : 0 : 0 \mid 1];$$

and the “centre” is at

$$[a_1; \dots : a_n \mid].$$

for all admissible sequences (a_1, \dots, a_n) with $a_n \neq 0$.

It is clear that the set is invariant under the multiplication of all the coordinates by any positive real number. Hence to get the structure of the non-convergence set it is sufficient to know the intersection of this set with the plane $x_1 + x_2 + x_3 = 0$.

In Figure 2 we show the first several removed triangles. They correspond to the sum of the elements of the Farey summation continued fractions smaller or equal to 3 and 4 respectively.

On the left figure we show the removed (corner) triangles. Dashed lines connect the vertices $(1, 0, 0)$, $(0, 1, 0)$, and $(0, 0, 1)$ to the “centre” points $[a_1; \dots : a_n |]$.

2.6.2 No guaranteed algebraic cubic periodicity of the Farey summation algorithm

First of all let us observe the following straightforward statement.

Proposition 2.44. *Let $v = (x, y, z)$ be a vector such that $0 < x < y < z$. Assume that the fraction for v contains only entries for A_1 and A_2 . Namely, it is equivalent to the following infinite sequence.*

$$[a_1; a_2 : 0 : a_3 : a_4 : 0 \dots |]$$

Then the regular continued fraction for y/x is $[a_1; a_2 : a_3 : a_4 \dots]$.

□

Now let us consider one particular example when cubic periodicity fails (that provides a counterexample to the Last Jacobi’s theorem for Farey summation algorithm).

Example 2.45. (Failure of algebraic cubic periodicity.) Consider the matrix

$$\begin{pmatrix} 10 & 0 & 1 \\ 1 & 10 & 0 \\ 0 & 1 & 0 \end{pmatrix}.$$

Its characteristic polynomial $t^3 - 20t^2 + 100t - 1$ is irreducible over \mathbb{Q} . Let us take the vector v corresponding to the maximal eigenvalues and with the last coordinate equal to 1:

$$v \approx (3.21113935\dots, 10.31141595\dots, 1).$$

The corresponding Farey summation continued fraction is

$$[0; 0 : 3 : 4 : 0 : 1 : 2 : 0 : 1 : 3 : 0 : 1 : 3 : 0 : 1 : 1 : 0 : 2 : 1 : 0 : 1 : 19 : \dots |],$$

which is not periodic, since the sequence of elements for this continued fraction coincide (after removing zeroes) to the regular continued fraction for the cubic number v_1/v_3 :

$$\frac{v_1}{v_3} = [3; 4 : 1 : 2 : 1 : 3 : 1 : 3 : 1 : 1 : 2 : 1 : 1 : 19 : \dots].$$

This continued fraction is not periodic by Lagrange’s theorem, since the ratio v_1/v_3 is not a quadratic irrational number.

3 Properties and invariants of Farey polyhedra

Now we come to the main section of the paper.

We start with a short discussion of the basic properties of the Farey tessellation. Then in Subsection 3.2 we introduce a central object of study, the combinatorial *prismatic diagram*. From these diagrams, in Subsection 3.3 we define a generalisation of the notion of sails and introduce the important invariants, the *LLS sequences*.

In Subsection 3.4 we study the matrix decomposition of the Farey summation algorithm, which is necessary for the study of LLS sequences in Subsection 3.5. The decomposition allows a simple definition of three-dimensional *continuants*, shown in Subsection 3.6.

We finish the section in Subsection 3.5 where we introduce *frieze patterns* from prismatic diagrams, and discuss the generating *Ptolemy relation* for frieze patterns.

3.1 Basic properties of Farey tessellation

Now it is time to formulate and prove the following general statements of the structure of the Farey tessellation of the positive orthant.

Proposition 3.1. *The following holds:*

- (i) *The union of all vertices of all Farey simplices (of all dimensions) is the intersection of the unit integer sphere with the positive orthant;*
- (ii) *The closure of the union of all the simplices is the positive orthant;*
- (ii) *The interiors of two distinct Farey simplices of maximal dimension do not intersect.*

Proof. (i) Consider $v \in \mathbb{Z}S^{n-1}$ in the positive orthant. The Meester algorithm for v will generate the Farey summation continued fraction. The corresponding nose stretching procedure for that continued fraction will produce a sequence of Farey simplices, such that the last one contains v as a vertex.

(ii) Consider any point v with non-rational coordinates and consider a sequence of elements $v_i \in \mathbb{Z}S^{n-1}$ whose directions converge to the direction of v . Then the closure of the union of segments Ov_i contains v in the closure. Finally note that Ov_i is covered by Farey simplices, where this covering is produced by the nose stretching procedure for v .

Since the set of v with irrational coordinates is everywhere dense, the closure of Farey simplices covers the whole positive orthant.

(iii) Let these simplices S_1 and S_2 be constructed by two distinct sequences of the Farey algorithm Λ_1 and Λ_2 . Let us consider the following cases:

- If Λ_1 starts from Λ_2 . Then let us pick the plane π of the last supporting simplex in Λ_1 . By construction the origin and S_1 are in one halfspace with respect to π while S_2 is in the other. Therefore, their interiors do not intersect.
- If Λ_2 starts from Λ_1 . This case is similar to the above one.
- Neither of the above two cases. This means that after some time the sequences of simplices projects to different non-intersecting triangles in the Farey net. Therefore they do not have a common point in their interiors.

□

We would like to continue with the following important example.

Example 3.2. Farey three-dimensional tessellation does not contain all empty tetrahedra of volume 2. Let

$$v_1 = (6, 14, 15), \quad v_2 = (5, 13, 14), \quad v_3 = (5, 12, 13),$$

and let $w = v_1 \oplus v_2 \oplus v_3 = (16, 39, 42)$.

The tetrahedra $wv_1v_2v_3$ is empty. The continued fraction of w is $[2; 1 : 2 : 0 : 3]_{1,3}$. The base triangle of the tetrahedron that has pennant w is formed from the vertices $[2; 1]$, $[2; 1 : 2]$, and $[2; 1 : 2 : 0 : 2]$. These are not the vertices v_1 , v_2 , and v_3 . The reason for this is that to reach any v_i we must use a two-dimensional step. Hence not all empty tetrahedra are contained in the three-dimensional Farey tessellation.

3.2 Prismatic triangulations

Now we study the combinatorial structure of Farey polyhedra.

3.2.1 Ordered path-triangulations and their complete invariant

In this section we consider *polyhedra* as convex hulls of finite numbers of points. We say that a polyhedron is *marked* if each of its edges contain a finite number of marked interior points (zero is also allowed). A decomposition of a marked polyhedron P into non-intersecting simplices (of maximal dimension) is said to be a *triangulation* of P if the set of vertices of all such simplices coincides with the union of all vertices of P and all marked points of P .

Recall that the *dual* graph of a triangulation is the graph whose vertices are labeled by simplices in the triangulation; an edge of the dual graph connects two vertices if and only if the corresponding two simplices share a face of codimension 1.

Definition 3.3. We say that two triangulations are *similar* if there is a one-to-one map between their simplices that provides equivalence of their dual graphs.

Below we study triangulations of the following type.

Definition 3.4. We call a triangulation T a *path-triangulation* if its dual graph is a path graph.

3.2.2 Decks, masts, yards, crow's nests, and pennants

Recall the definitions of Subsection 2.3. In order to remove some natural symmetries of path-triangulations we introduce the following definition.

Definition 3.5. Consider a path-triangulation T . Let us mark by S_0 and S_1 the two simplices corresponding the endpoints of the dual graph, and let F_0 and F_1 be one of the codimension 1 *exterior* faces of S_0 and S_1 respectively, (i.e. F_0 and F_1 are not faces of some simplex other than S_0 and S_1). We say that T is *ordered* if the faces (F_0, F_1) are fixed and the vertices of F_0 are ordered. We say that F_0 is *deck* of T , and that F_1 is the *nest* of T (or *crow's nest*). The unique vertex of the nest that is not a vertex of any other simplex is called the *pennant*.

As we show later the nest has a natural ordering induced by the ordering of its deck (see Remark 3.10 below).

Definition 3.6. We say that an edge of an ordered path-triangulation is a *mast edge* if it is adjacent to a single simplex of maximal dimension and does not belong either to the deck or the nest of the triangulation.

An edge is said to be a *yard edge* if it is adjacent to more than one simplex of the triangulation.

A connected component of the union of edge masts is called a *mast*. A $k-1$ -dimensional face belonging to several simplices is called a *yard*.

Example 3.7. Figure 3 below shows a combinatoric representation of two-dimensional Farey summation continued fractions. On these diagrams, the deck and nest are represented by grey edges, and the masts by the exterior edges. The interior diagonals are yard edges (in two dimensions yards and yard edges coincide)

Proposition 3.8. *The following statements hold:*

- *Each simplex that is not the deck or the nest has precisely one mast edge;*

- Any mast is a broken line;
- One endpoint of any mast is at the deck and another is at the nest;
- Any vertex of the nest/deck has at most one mast adjacent to it with one exception. If a vertex of a deck is a vertex of a nest, then no mast are adjacent to this vertex.

Proof. Each simplex that is not the deck or the nest of the triangulation contains two faces of codimension 1 that are yards. The union of their edges are all edges of the simplex but one. This concludes the proof of the first item.

We prove the second, third, and fourth items simultaneously by induction on the number of simplices in the triangulation.

Base of induction. All the statements hold for a single simplex triangulation. It has a deck, a nest, and a single mast edge between the vertex of a deck that is not in the nest and a vertex of the nest that is not in the deck.

Step of induction. Let the statement hold for all triangulations on $n-1$ simplices. Consider any triangulation T of n simplices. The last simplex S_n of this triangulation has the nest N and one yard Y . Let D denotes the deck of T .

Let us remove S_n and consider the last yard Y as the nest of a smaller triangulation T' . All the statements hold for T' . Let us now add S_n . The last mast edge connects N and Y . Therefor:

- All mast are broken lines, as we add the last edge to the vertex where either only one mast or no masts.
- We either have changed only one endpoint of masts, which will have vertex in the nest N , or we create a new mast, then the corresponding vertex of Y should have been a vertex of the deck D by the induction assumption.
- Finally T and T' has the same deck D and the nests Y and N different by one vertex connected by a new edge. Hence the last statement holds.

That concludes the proof of the last three items. □

Proposition 3.8 allows us to give the following definition.

Definition 3.9. The set of masts admits an *induced ordering* by the indices of the first vertices in the masts (which is in the deck D with ordered vertices).

Remark 3.10. In particular the induced ordering of masts implies the ordering on the nest. Informally speaking, masts have a flavour of the notion of the parallel transform in differential geometry.

3.2.3 Prismatic polygons and diagrams

Definition 3.11. Let \mathcal{R}^{k-1} be a simplex of dimension $k-1$ with enumerated vertices R_1, \dots, R_k . Let v be a non-zero vector orthogonal to the plane R_1, \dots, R_k . Let also $D = (d_1, \dots, d_k)$ be a collection of non-negative integers. A *prismatic polyhedron* is a marked polyhedron

$$\text{conv}(R_1, \dots, R_k, R_1 + d_1 v, \dots, R_k + d_k v),$$

where at each edge $(R_i, R_i + d_i v)$ all the points $R_i + k v$ with $1 \leq k \leq d_i - 1$ are marked. We denote it by $(\mathcal{R}^{k-1}, v, D)$.

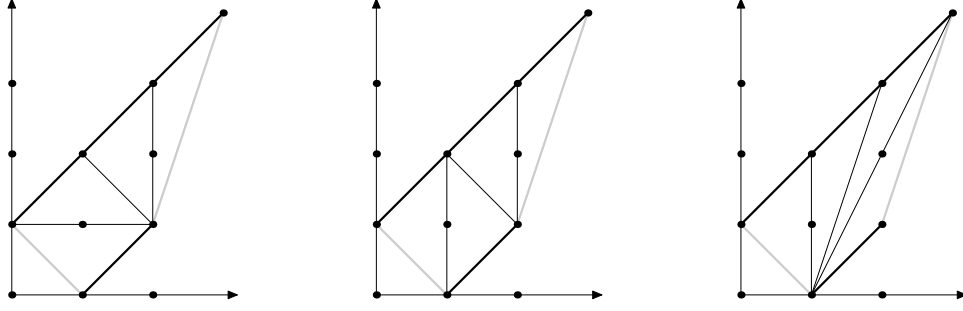


Figure 3: Triangulated canonical prismatic diagram

For any triangulation of the prismatic polyhedron we mark the faces

$$F_0 = (R_1, \dots, R_k), \quad \text{and} \quad F_1 = (R_1 + d_1 v, \dots, R_k + d_k v);$$

we order the vertices of faces as indices of R_i . Any ordered triangulation (with marked faces F_0 and F_1 as above) of a prismatic polygon is called a *prismatic diagram*.

In the two-dimensional case the canonical prismatic diagram is also known under the name *Farey boat*, based on the terminology from [40].

Definition 3.12. A prismatic diagram is said to be *canonical* if \mathcal{R}^{k-1} is the tetrahedron whose vertices are the endpoints of the first k coordinate vectors and $v = (1, 1, \dots, 1, 0, 0, \dots, 0)$, where the number of unit coordinates is k .

Definition 3.13. Consider a canonical prismatic triangulation \mathcal{D} of length n and dimension k . The *LR-sequence* of \mathcal{D} is the following sequence of indices in $\{1, \dots, k\}$ of length n :

$$(M_1, \dots, M_n),$$

where $M_i \in \{1, \dots, k\}$ denotes the index of a mast that we build on Step i .

Recall that the masts are ordered $(1, \dots, k)$: at each Step i of the Farey summation algorithm we add a single mast edge to one of the masts. The index of the addended mast is collected as M_i .

Remark 3.14. In particular we can write the LR-sequence in the exponential form:

$$1^{a_1} 2^{a_2} \dots k^{a_k} 1^{a_{k+1}} \dots$$

for some non-negative collection of a_i . This expression provides a link to theory of continued fractions, which we explore in this paper for the particular case of Farey summation continued fractions. (It can be applied to other additive algorithms as well.)

Example 3.15. In Figure 3 we show the three triangulations of the prismatic polygons in two dimensions with $D = (1, 3)$. The decks and nests are shown in grey. The masts are shown in bold. The LR-sequences from left to right are $(1, 2, 2, 2)$, $(1, 2, 1, 1)$, and $(1, 1, 1, 2)$ or, in exponential form, $(1^1, 2^3)$, $(1^1, 2^1, 1^2)$, and $(1^3, 2^1)$, respectively. The pennant is the point $(3, 4)$ in each diagram.

Remark 3.16. Canonical prismatic diagrams generalise the Farey boats introduced by S. Morier-Genoud and V. Ovsienko in [40] to higher dimensions. The prismatic diagrams in Figure 3 are exactly the Farey boats (also called *wrinkled triangulations*), after transformation of vertices by

$$\begin{pmatrix} 0 & 1 \\ -1 & 1 \end{pmatrix}.$$

The prismatic diagrams give a combinatorial description of Farey polyhedra. In two dimensions they link to the theory of cluster algebras through their relation to Conway-Coxeter friezes. The connection between frieze patterns and triangulated polygons was found by J. Conway and H. Coxeter in [12], and the connection to cluster algebras by P. Caldero and F. Chapoton [11].

The following statement is now straightforward.

Corollary 3.17. *The LR-sequence is an invariant of similarity of ordered path-triangulations.*

Let T be a path-triangulation of a k -dimensional polyhedron. Let us describe a natural piecewise linear map to the canonical prismatic diagram T .

- First of all we map the deck of T linearly to the triangle $E_1 \dots E_k$.
- Secondly we map the masts linearly to the corresponding lines $E_i + tv$ parameterised by t . The map is linear at each mast edge, and it sends consecutive vertices to consequent points $E_i + jv$ where $j = 1, 2, \dots$
- Finally, once the images of all simplices are defined, we map them linearly as well.

Definition 3.18. The prismatic polygon constructed above is said to be *associated* to a path-triangulation T .

The associated polygon has an induced structure of an ordered triangulation, which we call the *canonical prismatic diagram* of T and denote by $\mathcal{D}(T)$.

Definition 3.19. We say that two prismatic diagrams are similar if there exists an affine map that preserves the triangulation and sends marked faces F_0 and F_1 from the first diagram to the marked faces F'_0 and F'_1 respectively (here our map must preserve the enumeration of vertices) of the second diagram.

Corollary 3.20. *The canonical prismatic diagram is a complete invariant of prismatic triangulations.*

Proof. Indeed any canonical prismatic diagram is an ordered triangulation, so all canonical diagrams appear.

It is also clear from construction that different canonical prismatic diagrams are not similar.

Finally the above construction shows that every ordered triangulation is similar to one of the canonical prismatic diagrams. \square

Remark 3.21. As a conclusion the LR-sequences is a complete invariant of canonical prismatic diagrams (and, equivalently, of similarity types of ordered path-triangulations). Hence the number of distinct canonical prismatic diagrams (of dimension k consisting of d simplices) coincides with the number of LR-sequences of length d , which is equivalent to k^d .

3.2.4 Prismatic flag diagrams

Definition 3.22. Let $P_1(\mathcal{R}^{k_1-1}, v_1, D_1)$ and $P_2(\mathcal{R}^{k_2-1}, v_2, D_2)$ be two prismatic polytopes such that $k_2 \leq k_1$. Let also $S \subset \{1, \dots, k_1\}$ be a k_2 element set of indices. The *concatenation of* $(\mathcal{R}^{k_1-1}, v_1, D_1)$ and $(\mathcal{R}^{k_2-1}, v_2, D_2)$ with respect to S is adding extra segments in the direction of the rays with indices $s_i \in S$ for $i = 1, \dots, k_2$:

$$[R_{1,s_i} + d_{1,s_i} v_1, R_{1,s_i} + d_{1,s_i} v_1 + d_{2,i} v_2],$$

where s_i is the i -th element of S . The resulting set is the union of the polytope P_1 and the convex hull of all the new added segments

$$P_1 +_S P_2.$$

We denote it by

$$(\mathcal{R}^{k_1-1}, v_1, D_1, (D_2, S)).$$

Definition 3.23. Now let us have a sequence of prismatic polytopes $P_j(\mathcal{R}^{k_j-1}, v_j, D_j)$ with $j = 1, \dots, l$ with $k_1 > k_2 > \dots > k_l$. Let also S_i be sets of indices of k_i elements such that $S_l \subset S_{l-1} \subset \dots \subset S_1$ (disregarding the orders of their elements). Here we assume $S_1 = (1, 2, \dots, k_l)$. The polytope

$$(\dots (P_1 +_{S_2} P_2) +_{S_3} P_3) +_{S_4} \dots +_{S_l} P_l.$$

is said to be a *prismatic flag polytope*. We denote it by

$$(\mathcal{R}^{k_1-1}, v_1, (D_i, S_i)_{i=1}^l).$$

Let now P_j have prismatic diagrams T_j for $j = 1, \dots, l$. The natural mapping of these triangulations to the prismatic flag polytope is said to be a *prismatic flag diagram*. We denote it by

$$(T_i, S_i)_{i=1}^l,$$

where $S_1 = (1, \dots, k)$.

In the case when T_1 is a canonical prismatic diagram, we say that the prismatic flag diagram is *canonical* as well.

Remark 3.24. Note that the concatenations of prismatic polytopes and their prismatic diagrams depend neither on the positions of tetrahedra R^{k_i-1} nor on vectors v_i for $i = 2, \dots, l$; it depends only on the dimensions k_i and the sets D_i (for $i = 2, \dots, l$) and on the first prismatic polytope (R^{k_1-1}, v_1, D_1) .

Remark 3.25. Finally it remains to say that, due to the freedom of the ordering of subsets S_i , there are several obvious ways to obtain the same canonical flag diagrams (by permuting S_i and the LR sequences of the corresponding T_i).

3.2.5 Canonical Prismatic flag diagrams and Farey summation continued fractions

Consider an extended Meester algorithm continued fraction:

$$\alpha = [a_1; \dots : a_{s_{j_1}} \mid_{j_1} a_{s_{j_1}+1} : \dots : a_{s_{j_2}} \mid_{j_2} a_{s_{j_2}+1} : \dots : a_{s_{j_{n-2}}} \mid_{j_{n-2}} a_{s_{j_{n-2}+1}} : \dots : a_N].$$

For every $i = 1, \dots, n-1$ we consider T_i be the canonical prismatic diagram, whose LR-sequence is $(a_{s_{j_{i-1}}+1}, \dots, a_{s_{j_i}})$. Here we allow the sequences to be empty. Finally let

$$S_1 = \{1, \dots, k\} \quad \text{and} \quad S_i = S_{i-1} \setminus \{j_i\} \text{ for } i = 2, \dots, n-1.$$

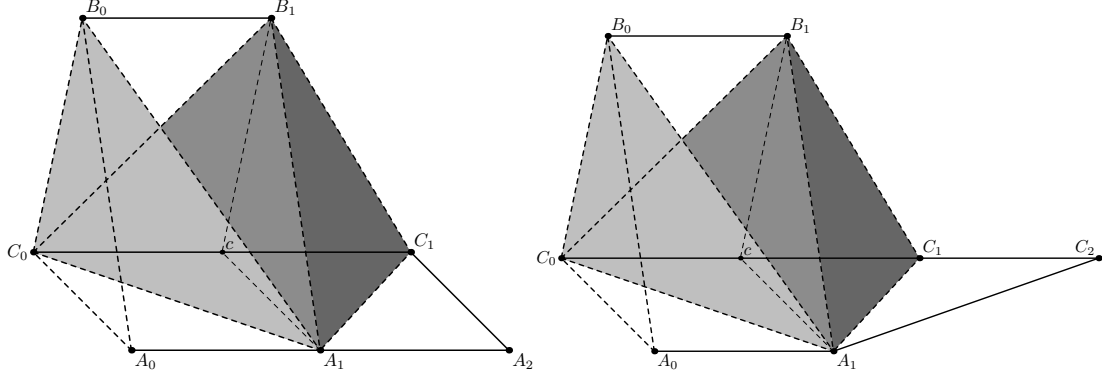


Figure 4: Two prismatic triangulations for $(5, 7, 8)$ corresponding to $[1; 1 : 2 |_2 1]$ (Left) and to $[1; 1 : 2 |_2 0 : 1]$ (Right).

Definition 3.26. We say that the canonical flag diagram $(T_i, S_i)_{i=1}^{n-1}$ constructed above is the *canonical prismatic flag diagram* for the Farey summation continued fraction α . We denote it by $T(\alpha)$.

Theorem 3.27. *The canonical prismatic flag diagrams form a complete invariant for Farey summation continued fractions. In addition the combinatorics of $T(\alpha)$ coincide with the combinatorics of the Farey polyhedron.* \square

Example 3.28. Let us show the prismatic triangulations for the vector $v = (5, 7, 8)$ of Example 2.26.

Note that we have two different continued fractions defined by $(5, 7, 8)$:

$$[1; 1 : 2 |_2 1], \quad \text{and} \quad [1; 1 : 2 |_2 0 : 1].$$

(Technically the algorithm will never arrive to the second continued fraction.)

The corresponding canonical prismatic flag diagrams are shown in Figure 4. They both consist of 4 simplices of dimension 3 and one simplex of dimension 1. The simplices of dimension 3 are

$$A_0B_0C_0A_1, \quad A_1B_0C_0B_1, \quad A_1B_1C_0c, \quad A_1B_1cC_1.$$

The simplices (triangles) of dimension 2 are $A_1C_1A_2$ and $A_1C_1C_2$ respectively.

Remark 3.29. The above construction has a straightforward generalisation to the case of infinite continued fractions. We omit it here.

3.3 Sails and their LLS sequences

In this subsection we discuss a generalisation of sails and LLS-sequences to the multidimensional case.

3.3.1 Sails of prismatic diagrams and Farey polyhedra

Definition 3.30. Let T be a canonical prismatic flag diagram in dimension n . Consider the hyperplane spanned by a codimension 1 face of the deck (we exclude the i -th vertex) and the

vector $(1, 1, \dots, 1)$. The intersection of T with this hyperplane is called the *sail* of the T and denoted $\text{sail}_i(T)$.

The intersection of the sail $\text{sail}_i(T)$ with the deck, the nest, masts, and yards are respectively the *deck*, the *nest*, the *masts*, and the *yards* of $\text{sail}_i(T)$.

Definition 3.31. The inverse image of the piecewise linear map (see Definition 3.18) between the union of the Farey polyhedron (equipped with its subdivision to Farey simplices) and the corresponding canonical prismatic flag diagram defines the *masts* of the Farey polyhedron. Recall that the deck/nest/yards/pennant are already stated in Algorithm 2.18.

In addition the inverse image defines *sails* of the Farey polyhedron and their *decks*, *nests*, *masts*, and *yards*.

Remark 3.32. The sail $\text{sail}_i(T)$ is the union of the simplices bound by all but the i -th mast, and the masts themselves. In two dimensions $\text{sail}_i(T)$ is simply the i -th mast. In this case we have a classical construction of sail, see e.g., in [22]. The earliest use of the term sail is from V. Arnold, see for instance [1]. The theory of geometric continued fractions was instigated by F. Klein in his papers [29, 30].

Three-dimensional *sails* for a ray v in the positive octant are the unions of pairs of masts together with the sequence of triangles joining them.

3.3.2 On the masts at the point of dimension drop

First let us assume that all of the simplices of the Farey summation continued fraction are of the same dimension k . Then all the mast edges are uniquely defined except for the last one. This happens since there is no natural way to define the nest combinatorially (without involving any ordering). So we can connect the last vector with any of the masts. In other words we have:

$$[a_1; a_2 : \dots : a_n] = [a_1; a_2 : \dots : a_n - 1 : 1] = [a_1; a_2 : \dots : a_n - 1 : 0 : \dots : 0 : 1].$$

where the number of zeroes does not exceed $k - 2$. This will represent precisely all possible choices of the nest and of the last element of the mast.

This corresponds to the phenomenon for classical continued fractions, where:

$$[a_1; a_2 : \dots : a_n] = [a_1; a_2 : \dots : a_n - 1 : 1].$$

Now if a canonical prismatic diagram consists of several parts of different dimensions, a similar situation occurs. Here, for each one of the masts that vanishes at this step, its indices should be connected to the first new point of the next part of the flag.

3.3.3 A rigid structure of Farey masts, nose stretching

If we elongate any edge of any mast by a unit length vector in the direction of the edge we will reach the first point of some edge on one of the other masts.

Remark 3.33. Informally speaking the structure of the Farey polyhedron is linearly rigid. It gives rise to various dualities of the sails. The fact that stretching a mast edge provides the starting point of a separate mast edge provides a very fast geometric construction of the Farey polyhedron.

Namely, we start with basis elements E_i ($i = 1, \dots, k$) and their sum P_1 . Then add the vector $E_1 P_1$ to E_1 , a_1 times. This will generate the first new vector of the Farey polyhedron (of course if $a_1 \neq 0$), which we denote by $E_{1,2}$.

Now we add E_1P_1 to $E_{1,2}$ once more to get P_2 , symbolically

$$\begin{aligned} E_{1,2} &= E_1 + a_1 E_1 P_1, \\ P_2 &= E_1 + (a_1+1) E_1 P_1. \end{aligned}$$

Now the point P_2 is on the first edge emanating from E_2 (except for the case $a_2 = 0$). So we set

$$\begin{aligned} E_{2,2} &= E_2 + a_2 E_1 P_2, \\ P_2 &= E_2 + (a_2+1) E_1 P_2. \end{aligned}$$

Proceeding further we will construct the whole Farey polyhedron. This procedure is called the *nose stretching* for prismatic diagrams. Informally, at each moment we stretch one of our k -noses further and further away.

Definition 3.34. The vertices $E_{i,j}$ generated by the algorithm are called the *partial quotients* of v .

Remark 3.35. Nose stretching exactly generalises the procedure for classical continued fraction theory. This procedure is specific to the Farey algorithm.

3.3.4 LLS-sequences and their dualities

Every sail possesses a collection of invariants that encodes most of the elements of the continued fractions. In this subsection we introduce the LLS-sequence. Let us start with a few notions used in the definition of the LLS-sequence.

An angle is *integer* if its vertex is an integer point. An angle is rational if both of its edges contain integer points distinct from the vertex.

Definition 3.36. Let π_1 and π_2 be two planes with a nonzero intersection. Let W be a basis for $\pi_1 \cap \pi_2$, and let U and V be complements of W to the bases of π_1 and π_2 respectively. Then the expression

$$\frac{\text{IV}(V, U, W)}{\text{IV}(V) \cdot \text{IV}(U) \cdot \text{IV}(W)}$$

is called the *integer sine* of the angle between π_1 and π_2 and denoted by $\text{lsin}(\pi_1, \pi_2)$.

Definition 3.37. Consider the sequence of principal simplices T_i constructed by the Farey summation algorithm for some integer vector. Let F_i be the intersection of a sail with the principal simplex T_i . Then we say that F_i is a *principal face of this sail* if $\dim F_i \geq \dim T_i - 1$. The set of all principal faces of a sail has a natural ordering induced by the ordering of the Farey summation algorithm.

A *mast segment* is the union of all mast edges in a line.

Remark 3.38. For the principal face there are the following two possibilities.

$$\dim F_i = \begin{cases} \dim T_i, & \text{if the } j\text{-th mast was removed before the } i\text{-th step;} \\ \dim T_i - 1, & \text{otherwise.} \end{cases}$$

Example 3.39. In Figure 4, for the sail between masts A and C , we see the principal faces are $A_0A_1C_0$, $A_1C_0C_1$, and $C_1A_1A_2$.

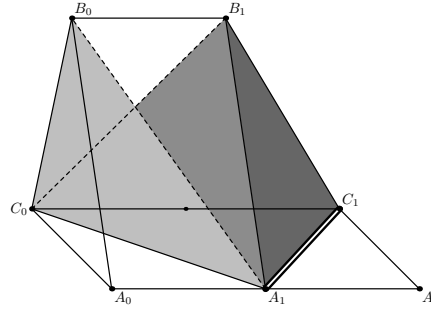
Definition 3.40. The LLS sequence of the j -th sail is the j -th sail of the canonical prismatic flag diagram equipped with the following:

- Each pair of consecutive principal faces is equipped with the integer sine between the planes that these faces span. We indicate the yard edge connecting both principal faces (edge of a principal yard) and equip it with the corresponding integer sine (a dashed line indicates 0 integer sine: in this case the principal faces lie in the same plane in the Farey polyhedron);
- We indicate the dropping of the j -th mast by a double yard edge.
- For the simplicity of drawing we replace mast segments of length n by a single segment of length 1 equipped with n (the integer length).

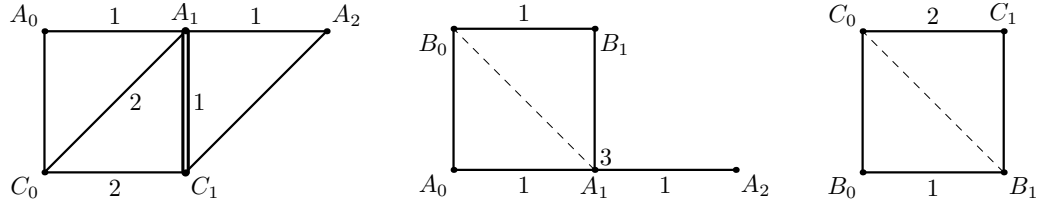
Remark 3.41. The term LLS-sequence (lattice length-sine sequence) comes from a similar notion in the two-dimensional case (see, for example, in [21, 22]). In the two-dimensional case we have a sequence of numbers, whereas in three dimensions the prismatic flag diagrams encode sequences of principal faces.

For consistency, let us start with our standard example.

Example 3.42. Let us start with the Farey polyhedron for $v = (5, 7, 8)$ of Example 2.26.



The sails opposite to masts B , A , and C have the following LLS-sequences.



The first sail is the most informative, it shows all the positive elements of the continued fraction $[1; 1 : 2 : 0 : 0 | 1]$. As we will see later in Proposition 3.45, the first element of the Farey summation continued fraction is the first number in the top row; the second element is a half of the first number in the middle row; the third element is the bottom one; the last element is the last in the top row.

In order to further understand the coefficients of the LLS-sequence we consider a longer example.

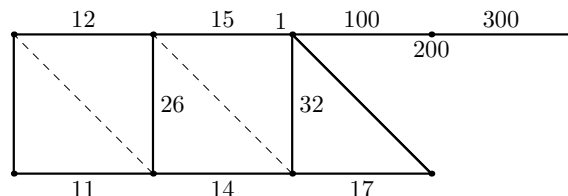
Example 3.43. Let us consider a vector

$$v = (1656812331613081, 18353000512178816, 19770900109601816).$$

Direct computation shows that its Farey summation continued fraction is

$$[11; 12 : 13 : 14 : 15 : 16 : 17 | 100 : 200 : 300 : 400].$$

The LLS-sequence of the sail for the first two masts is as follows:



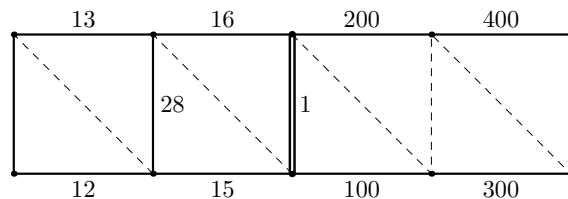
Here the first mast is the bottom one, the second mast is the top one. We write the corresponding integer lengths near the corresponding mast segments.

The non-horizontal segments with numbers indicate the common faces of two consecutive principal faces, the numbers are the corresponding integer sines of the angles between the planes.

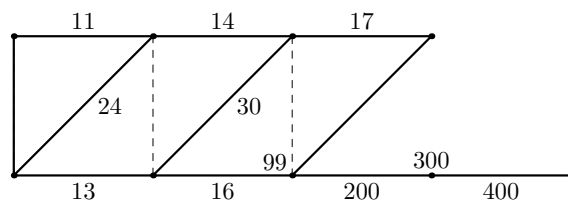
Finally, dashed lines correspond to the yards joining the endpoints of the mast segments of the same principal face. (They indicate the order in which the continued fraction should be taken, here we add triangles from the left to the right, the middle numbers go first.)

The elements of the Farey summation continued fraction of index $3i + 1$ are on the first mast; of index $3i + 2$ are on the second. In order to get the remaining elements, we divide the sequence of integer sines by the dimension of the smallest adjacent principal face, i.e. $26/2$, $32/2$, and $200/1$.

Let us write the LLS-sequences for the other two sails. The LLS-sequence for the sail with the second and the third masts is as follows:



Finally the LLS-sequence for the sail with the third and the first masts is



Remark 3.44. As we see the LLS-sequences contain information on most of the elements of the continued fraction (except for the few first and last elements) This situation is similar to the classical case. It is due to the duality discussed in the next proposition.

We say that the sail *opposite* to a given mast is the sail that does not contain this mast.

We say that two mast segments on different sails of the Farey polyhedron are *neighbours* if the lines containing them intersect. As we know from Subsection 3.3.3 every mast segment contains precisely two neighbours (except for the first one and for the last one).

Proposition 3.45. (On duality of integer lengths and integer sines in sails.) *Consider a mast segment M and let π_1 and π_2 be the planes of the principal faces of the opposite sail that contain neighbouring segments. We assume that the dimensions of π_1 and π_2 are both equal to k . Then the integer length of the mast segment M multiplied by k is the integer sine of the angle between π_1 and π_2 ,*

$$\text{lsin}(\pi_1, \pi_2) = k \cdot \ell(M).$$

Proof. The proof is straightforward. Any two consecutive planes in some coordinates are equivalent to two planes of a short Farey summation continued fraction formed only by 3 positive elements, say (a, b, c) .

Note that the elements a and c correspond to the some mast segments of the sail, while b corresponds to some mast segment of the opposite mast. There are only two different cases here (up to re-numeration of basis vectors): either the mast segments for a and c are on the same mast or not.

In both cases direct computations show that the integer sine equals kb . This concludes the proof. \square

We discuss the three-dimensional case in more detail (including the cases of different dimensions of faces) in Subsection 3.5 after we introduce the matrix form.

3.4 Semi-group of matrices by multiplication

The multidimensional Farey summation algorithm can be described by matrix multiplication. At each step we multiply by a certain matrix. In this subsection we continue with the three-dimensional case in order to simplify the exposition. Nevertheless most of the definitions, notions, and statements have a straightforward generalisation to the multidimensional case.

3.4.1 Matrices associated to the steps of the algorithm

The algorithm begins in Stage 1 with two-dimensional yards; at that stage we employ the matrices:

$$A_1 = \begin{pmatrix} 1 & 0 & 0 \\ 1 & 1 & 0 \\ 1 & 0 & 1 \end{pmatrix}, \quad A_2 = \begin{pmatrix} 1 & 1 & 0 \\ 0 & 1 & 0 \\ 0 & 1 & 1 \end{pmatrix}, \quad \text{and} \quad A_3 = \begin{pmatrix} 1 & 0 & 1 \\ 0 & 1 & 1 \\ 0 & 0 & 1 \end{pmatrix}.$$

Once we arrive at one-dimensional yard (i.e. to Stage 2) we continue with matrices

$$B_{ij} = \text{ld} + E_{i,j}, \quad \text{for } 1 \leq i, j \leq 3 \text{ and } i \neq j.$$

Here ld is the identity matrix and $E_{i,j}$ is a matrix with only one non-zero entry at place (i, j) which is equal to 1.

3.4.2 Partial quotients

Let us continue with the notion of partial quotients.

Definition 3.46. Let $\alpha = [a_1 : \dots : a_n | b_1 : \dots : b_m]$ be a continued fraction. Consider the matrix

$$M = A_1^{a_1} A_2^{a_2} A_3^{a_3} A_1^{a_4} \dots A_k^{a_k} B_{st}^{b_1} B_{ts}^{b_2} B_{st}^{b_3} B_{ts}^{b_4} \dots,$$

where $s, k \in \{1, 2, 3\}$ such that $s = k+1 \pmod{3}$, $t = k+2 \pmod{3}$. We say that the vectors of M form the integer basis *associated* with the continued fraction. We say that the matrix M is the *continued fraction matrix* and denote it by $M(\alpha)$.

Remark 3.47. The matrix decomposition of Definition 3.46 is extremely important. It provides an analytic continuation of the Farey summation algorithm to the case of arbitrary real elements. In the above definition one can take arbitrary real numbers (a_i) and (b_j) , as these powers are well-defined for the matrices. Here one should replace the non-zero off-diagonal elements by the corresponding (a_i) and (b_i) ; e.g.

$$A_1^{a_1} = \begin{pmatrix} 1 & 0 & 0 \\ a_1 & 1 & 0 \\ a_1 & 0 & 1 \end{pmatrix}.$$

Remark 3.48. We would like to stress that the matrix multiplication order for Farey summation algorithm is as in Definition 3.46 and not the inverse one.

Remark 3.49. Finally, note that we use the Farey summation continued fraction here, and not the Meester algorithm continued fraction (the difference is simply in the number and position of certain zeroes in the continued fraction).

Definition 3.50. Let α be some continued fraction and let α_i be the continued fractions defined by the first i elements of α . We say that α_i is the i -th partial quotient of α , and call $M(\alpha_i)$ the i -th partial quotient matrix and denote it by $M_i(\alpha)$.

Proposition 3.51. Let α be a continued fraction for v . Then the partial quotient matrix $M_i(\alpha)$ contains all the vectors of the i -th yard as columns. \square

In particular if we have the following statement.

Corollary 3.52. Let α be a finite continued fraction for v . Then the continued fraction matrix $M(\alpha)$ contains the vector v as a column. \square

Remark 3.53. It turns out that matrices A_1 , A_2 , and A_3 form a free generated semi-group (as they correspond to different triangles in the tessellation). Their products applied to $(1, 0, 0)$ generate all integer vectors v of $\mathbb{Z}S^2$ whose continued fraction have empty sequence (b_i) . It is clear that we cannot obtain vectors of $\mathbb{Z}S^2$ that have a non-zero (b_i) sequence. For instance, $v = (6, 14, 15)$ from Example 3.2 is one of such vectors, it has continued fraction $[2; 1 : 2 | 2 : 0 : 0 : 2]$.

We arrive to the following natural question.

Problem 1. Describe the set of matrices $M(\alpha)$ where α has a finite sequence (a_i) and an empty sequence (b_j) .

Remark 3.54. Now we have a simple way to compute all Farey simplices for the given vector v . First of all the Meester algorithm produces the continued fraction $\alpha(v)$ for v . Secondly the matrices $M_{i-1}(\alpha(v))$ and $M_i(\alpha(v))$ provide all the vertices of the i -th Farey simplex for v . Here the matrix $M_{i-1}^{-1}(\alpha(v)) \cdot M_i(\alpha(v))$ tells us which columns are in the simplex (This matrix is either one of the A or B matrices in position i of the decomposition of Definition 3.46.)

Remark 3.55. The matrix multiplication introduced in this subsection can be extended to the higher dimensional cases in a straightforward way. Since we mostly work in the three dimension case in what follows, we skip the multidimensional notation here.

Example 3.56. Consider $v = (5, 7, 8)$ from Example 2.26. As we know from Example 2.30, the continued fraction for $(5, 7, 8)$ is

$$\alpha(v) = [1; 1 : 2 : 0 : 0 | 1].$$

Hence

$$M(\alpha(v)) = A_1 A_2 A_3^2 A_1^0 A_2^0 B_{31}.$$

It is interesting to note that v can be alternatively obtained from $[1; 1 : 2 : 0 : 0 | 0, 1]$

3.5 LLS-sequence in the three-dimensional case

In this subsection we discuss the three-dimensional LLS sequence in more detail.

3.5.1 Values of integer sines in the LLS-sequence

Let us discuss how to get the values of the elements of the Farey continued fraction from LLS sequences. Without loss of generality we consider the sail defined by the first and the third masts. The integer lengths of the segments for the first and the third masts are shown on the top and the bottom horizontal lines of the sails representing masts 1 and 3; they provide nearly two thirds of all the elements of the continued fraction. We should learn how to read the elements represented by integer lengths of mast 2, which is not presented in our sail. Most of the elements of the second mast are reconstructable from the elements of the LLS sequence connecting the masts 1 and 3. These elements are integer sines of two consecutive faces of the corresponding sail. Such faces are generated by two, three, or four consecutive division tetrahedra (see Definition 2.22). In fact, four consecutive division tetrahedra are needed only in a very specific case when we drop dimension (represented in line 7 of Table 1 below); that might happen at most once for every continued fraction. We have the following different situations for the values of integer sines (without loss of generality we list only the cases when we start with mast 1):

In Table 1 we show schematically a part of the matrix decomposition for a continued fraction and the corresponding part of the LLS-sequence. Here the bottom and the top horizontal lines correspond to masts 1 and 3 respectively. Note that the integers a , b , x , and y in the table are assumed to be positive.

In the first two lines of the table there are no division tetrahedra representing the elements of mast 2; here the values on the sail-yards are either 0 or 1.

In the next two lines we generate the most common steps when the dimension is not dropped. In the third line we get the case of three-dimensional division tetrahedra where the value of the integer sine is $2x$. In the fourth line we show the two-dimensional division tetrahedra with the value of the integer sine being equal to x . This repeats the case of the classical two-dimensional LLS-sequence.

Further in lines 5 and 6 we have two cases where the algorithm loses one dimension but the elements of the continued fractions are still visible on the sail.

Finally in the last three lines we have the cases when we lose information on one or two of the elements.

Let us collect the above observations in the following theorem.

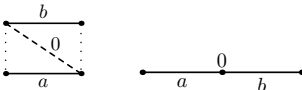
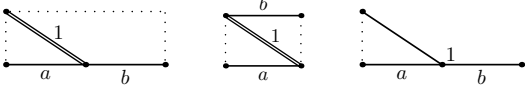
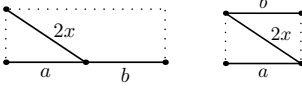
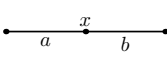
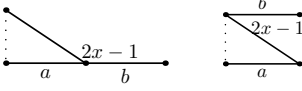
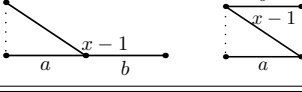
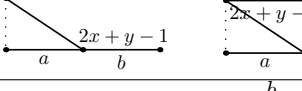
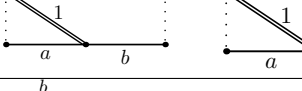
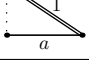
Theorem 3.57. *The three-dimensional LLS-sequence is an integer invariant of prismatic diagrams (and hence, by Theorem 3.27, also of Farey polyhedra).*

Proof. Note that the values of the LLS-sequence are completely given by the integer lengths of masts and the combinatorics of prismatic diagrams. Here the integer sines of the LLS-sequence are written in terms of the opposite mast, as in Table 1 (see also Proposition 3.45). \square

Remark 3.58. Recall that the powers in the matrix form coincide with integer length of the elements in the corresponding masts.

Remark 3.59. The situation is similar in four and higher dimensions. The number of cases will be finite but growing rather fast with the dimension. We omit the exhaustive study of all the cases here.

Table 1: Matrix decomposition and the corresponding values of the LLS-sequences.

Matrix decomposition	part of the LLS-sequences	lsin
$A_1^a A_3^b, \quad B_{13}^a B_{31}^b$		0
$A_1^a B_{13}^b, \quad A_1^a B_{31}^b, \quad A_1^a B_{12}^b$		1
$A_1^a A_2^x A_1^b, \quad A_1^a A_2^x A_3^b$		$2x$
$B_{12}^a B_{21}^x B_{12}^b$		x
$A_1^a A_2^x B_{12}^b, \quad A_1^a A_2^x B_{32}^b$		$2x - 1$
$A_1^a B_{21}^x B_{12}^b, \quad A_1^a B_{23}^x B_{32}^b$		$x - 1$
$A_1^a A_2^x B_{21}^y B_{12}^b, \quad A_1^a A_2^x B_{23}^y B_{32}^b$		$2x + y - 1$
$A_1^a A_2^x B_{13}^b, \quad A_1^a A_2^x B_{31}^b$		1
$A_1^a B_{32}^x B_{23}^b$		1

3.5.2 Integer arctangent of cones in three dimensions and sails

As we have seen, in the last three cases of the table the LLS-sequence does not catch x . However the integer invariants of the sail still encode x . First we need to set some further integer invariants.

A *cone* is the convex hull of three rays sharing a vertex. We call the rays the *edges of the cone*. A cone is *integer* if its vertex is integer. An integer cone is *rational* if each of its rays contains integer points distinct from the vertex.

Definition 3.60. Let α be a rational cone. Then there is an integer basis in which the vectors of α form (as columns) a matrix

$$\begin{pmatrix} 1 & a_1 & b_1 \\ 0 & a_2 & b_2 \\ 0 & 0 & b_3 \end{pmatrix}$$

satisfying $a_2 > a_1 > 0$, $b_3 > b_1 \geq 0$, and $b_3 > b_2 \geq 0$. Such a matrix is uniquely defined. It is called the *integer arctangent* of the cone, while its elements are said to be *integer sines* and *integer cosines*, labelled as follows:

$$\begin{pmatrix} 1 & \text{lcos}_{1,2} \alpha & \text{lcos}_{1,3} \alpha \\ 0 & \text{lsin}_1 \alpha & \text{lcos}_{2,3} \alpha \\ 0 & 0 & \text{lsin}_2 \alpha \end{pmatrix}.$$

(For further information, including the higher dimensional case, see [7]).

Note that the integer arctangent of α coincides with the Hermite normal form of the matrix of unit vectors generating the edges of α . All the coefficients of this matrix are integer invariants of the cone.

3.5.3 Application to sails

Let us go back to the last three lines of the table. More precisely we illustrate the case $A_1^a A_2^x B_{23}^y B_{32}^b$ of line 7.

As we see, the integer sine in the LLS-sequence provides us the value $2x + y - 1$ for the elements x and y (these are the lengths of mast segments of mast 2 which is not in our sail). Our aim is to construct an integer invariant of the sail that will provide us another equation on x and y .

Consider the simplicial cone α on the vectors generated by:

- the first segment of mast 1;
- the yard segment connecting the endpoint of the first segment of mast 3 with the second vertex of mast 1;
- the first segment of mast 3.

(All these edges are in the sail opposite to the second mast.) By the definition the arctangent of α is

$$\begin{pmatrix} 1 & 0 & x + 1 \\ 0 & 1 & x + y - 1 \\ 0 & 0 & 2x + y - 1 \end{pmatrix}.$$

From the last column we have:

$$\text{lcos}_{1,3} \alpha = x + 1, \quad \text{lcos}_{2,3} \alpha = x + y - 1, \quad \text{lsin}_2 \alpha = 2x + y - 1.$$

Remark 3.61. In particular $\text{lsin}_2 \alpha$ is the value that we have computed for the LLS-sequence, while the $\text{lcos}_{1,3} \alpha$ provides the value of x .

3.6 Continuants

In this subsection we briefly discuss the notion of continuants for Farey summation continued fractions.

Most Jacobi-Peron algorithms are defined by a linear recursion. In the case of the Farey summation algorithm we have the following recursion:

$$\begin{aligned} v_1 &= (1, 0, 0); & v_2 &= (0, 1, 0); & v_3 &= (0, 0, 1); \\ v_{i+3} &= v_i + a_i(v_{i+1} + v_{i+2}) & \text{for } i &= 1, 2, \dots \end{aligned} \tag{1}$$

This rule give rise to special functions that are called *continuants*.

In general, most continued fraction algorithms based on matrix multiplication generate their own (natural) notion of continuant. It is done as follows.

Firstly one fixes the generating family of matrices $S(k)$ (or sometimes several families) parameterised by a non-negative integer parameter k . In the case of Farey summation continued fractions that is

$$S(n) = \begin{pmatrix} n & 1 & 0 \\ n & 0 & 1 \\ 1 & 0 & 0 \end{pmatrix}.$$

Here the matrix $S(n)$ is a composition of A_1^n and a permutation of basis vectors.

Further we fix the following notation:

$$M_n(a_1, \dots, a_n) = \prod_{i=1}^n S(a_i).$$

Set also

$$v_n(a_1, \dots, a_n) = M_n(a_1, \dots, a_n) \cdot (1, 0, 0)^\top.$$

The coefficients of M_n in variables (a_1, \dots, a_n) are used to determine the continuants. That is suggested by the following two obvious relations on the coefficients of M_n :

- *recursive relation*: $M_n(a_1, \dots, a_n) = M_{n-1}(a_1, \dots, a_{n-1}) \cdot S(a_n)$;
- *anti-recursive relation*: $M_n(a_1, \dots, a_n) = S(a_1)M_{n-1}(a_2, \dots, a_n)$.

We synthesise the continuants as follows.

Definition 3.62. We define the n -th Farey continuant iteratively

$$\begin{aligned} K_0 &= 1; \\ K_1(x_1) &= x_1; \\ K_2(x_1, x_2) &= (x_1 + 1)x_2; \\ K_n(x_1, \dots, x_n) &= x_n(K_{n-1}(x_1, \dots, x_{n-1}) + K_{n-2}(x_1, \dots, x_{n-2})) + K_{n-3}(x_1, \dots, x_{n-3}). \end{aligned}$$

Example 3.63. Continuants of integer sequences are integers. For instance

$$\begin{aligned} K(2, 3, 4) &= 45, \\ K(15, 2, 4, 32, 54, 7) &= 2800350. \end{aligned}$$

The recursive and anti-recursive relations imply the following expression for all the coefficients of M_n in terms of continuant functions.

Remark 3.64. Note that, unlike in the two-dimensional case, we do not have the reverse symmetry for continuants:

$$K_n(x_1, \dots, x_n) \neq K_n(x_n, \dots, x_1)$$

Instead, from a simple inductive argument we find a separate recursive formula:

$$K_n(x_1, \dots, x_n) = x_1 K_{n-1}(x_2, \dots, x_n) + x_2 K_{n-2}(x_3, \dots, x_n) + K_{n-3}(x_4, \dots, x_n).$$

Proposition 3.65. *We have*

$$M_n(a_1, \dots, a_n) = \left(v_n(a_1, \dots, a_n), v_{n-1}(a_1, \dots, a_{n-1}), v_{n-2}(a_1, \dots, a_{n-2}) \right),$$

where

$$v_i(a_1, \dots, a_i) = \begin{pmatrix} K_i(a_1, \dots, a_i) \\ a_1 K_{i-1}(a_2, \dots, a_i) + K_{i-2}(a_3, \dots, a_i) \\ K_{i-1}(a_2, \dots, a_i) \end{pmatrix}.$$

Proof. The expression for M_n in terms of v_n , v_{n-1} and v_{n-2} follows from the recursive relation. The expression of v_i via continuants is a consequence of the anti-recursive relation. \square

Remark 3.66. Note that

$$v_n(a_1, \dots, a_n) = [a_1; \dots : a_n |].$$

Remark 3.67. The above is entirely related to Stage 1 (namely to matrices A_1, A_2, A_3). Stage 2 for B_{ij} employs classical continuants.

Example 3.68. Not all integer vectors of unit length are reached by continuants. As we have seen before, we sometimes need to use multiplication with B_{ij} matrices (see Example 3.2.)

Proposition 3.69. *Consider an integer point p with positive coordinates and with unit integer distance to the origin. Let us assume that*

$$p = v_n(a_1, \dots, a_n)$$

for some non-negative integers a_i (no two zeroes in a row except possibly at the start, $a_n \geq 2$). Then we also have

$$p = v_{n+1}(a_1, \dots, a_n-1, 1) = v_{n+2}(a_1, \dots, a_n-1, 0, 1).$$

Proof. This follows directly from the fact that the tetrahedra in the tessellation do not intersect. \square

Remark 3.70. As we see in the case of existence there are exactly three entirely three-dimensional Farey summation continued fractions representing p . The lengths of these continued fractions are three consecutive integers. This is similar to the classical two-dimensional case. In fact a similar statement holds in the multidimensional case (we omit it here).

3.7 Three-dimensional frieze relation

Frieze patterns are tables of numbers that encode the combinatorics of polygon triangulations. In this subsection we say a few words on a construction similar to frieze patterns in the classical case. Here we restrict ourselves to the case of three-dimensional Farey summation continued fractions that do not have zero elements. We are dealing with the three-dimensional part of the continued fraction only. We also consider only path triangulations for the polyhedra that admit path triangulations.

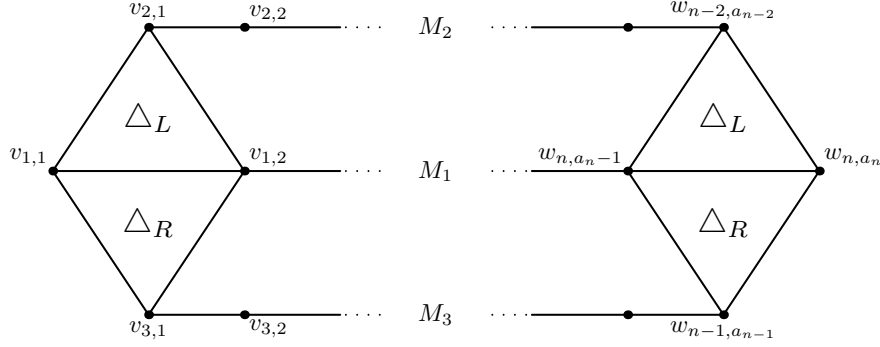


Figure 5: Left (\triangle_L) and right (\triangle_R) triangles at the beginning and end of the $(1, n)$ -slice.

3.7.1 Definition of λ -lengths

The tetrahedra in a prismatic diagram have a natural ordering. This ordering is defined by the intersection of these tetrahedra with the ray starting at the center of mass of the deck R and in the direction of v . We say that the number of tetrahedra in the prismatic diagram is the *length* of the prismatic diagram.

Definition 3.71. We say that a polyhedron is an (i, j) -slice of a prismatic diagram of length n if it is obtained from the diagram by removing all $i - 1$ simplices before the i -th yard and all $n - j$ simplices after the j -th yard. The i -th and j -th yards are called respectively the *deck* and *nest* of the (i, j) -slice.

Definition 3.72. Let P be a prismatic diagram. Consider two vertices (v, w) in P . We say that the *geodesic* $\ell(v, w)$ between two vertices of P is the smallest (i, j) -slice that contain these two points.

Definition 3.73. Since $\ell(v, w)$ is a path-polyhedron it naturally defines a Farey summation continued fraction $F(v, w)$ (as discussed above). We say that the *continuant* of this continued fraction is the λ -length of the geodesic $\lambda(v, w)$. We set $\lambda(v, v) = 0$. We also set $\lambda(v, w) = 1$ if $v \neq w$ and they are connected by a yard edge.

3.7.2 Ptolemy relation

Consider the triangulation of the boundary of the prismatic diagram.

Definition 3.74. We say that a face F is *nice* if it is neither a deck nor contains a vertex of the nest.

Definition 3.75. We call a face of a prismatic diagram a *left triangle* (\triangle_L) if two vertices are on mast m and one vertex is on mast $m + 1 \pmod 3$. Similarly we call a face a *right triangle* (\triangle_R) if two vertices are on mast m and one vertex is on mast $m - 1 \pmod 3$. See Figure 5 for reference.

The *Ptolemy relation* for prismatic diagrams in two dimensions is defined for pairs of edges of the diagram (cf. [40]): if (a_1, \dots, a_n) is the exponential form of the LR sequence of the minimal polygon containing two edges in the prismatic diagram then the Ptolemy relation is the determinant equation

$$\det \begin{pmatrix} K_n(a_1, \dots, a_n) & K_n(a_1, \dots, a_{n-1}) \\ K_n(a_1 - 1, \dots, a_n) & K_n(a_1 - 1, \dots, a_{n-1}) \end{pmatrix} = \begin{cases} 1, & n \text{ even;} \\ -1, & n \text{ odd,} \end{cases}$$

where K here denotes the two-dimensional continuant. The values in the matrix are the λ -lengths of pairs of vertices of the distinct edges.

Remark 3.76. Note that the values of the above matrix are exactly elements of the frieze pattern corresponding to the triangulated polygon. The -1 occurs precisely when the initial vertex and pennant of the (i, j) -th slice are on the same mast. This is explained by the difference between our ordering of vertices and the ordering in the classical correspondence between triangulated polygons and frieze patterns (see, for example, [40]).

In the three-dimensional case we define the Ptolemy relation for pairs of nice triangles (the faces on the boundary of the prismatic diagram).

Definition 3.77. Consider an ordered pair of nice triangles $V = v_1v_2v_3$ and $W = w_1w_2w_3$ not connected by a yard: V is ordered clockwise and W is ordered counter-clockwise. Then the *Ptolemy constant* for the pair (V, W) is $\det(\lambda(v_i, w_j))$. Denote it by $P(V, W)$.

Definition 3.78. We label the vertices of the prismatic diagram in the following way: for the exponential LR sequence (a_1, \dots, a_n) we label the vertices on the masts by $v_{i,j}$, where $0 \leq j < a_i$, and $v_{i,j}$ denotes the j -th vertex on mast segment associated to a_i (as in Definition 2.28).

Note that vertices connecting the two mast segments i and j are labelled twice, as v_{i,a_i} and $v_{j,1}$.

Proposition 3.79. Let (a_1, \dots, a_n) be the exponential form of the LR sequence for $\ell(v_{1,1}, w_{n,a_n})$. Then for the left and right triangles in $\ell(v_{1,1}, w_{n,a_n})$ with vertices $v_{1,1}$ and w_{n,a_n} we have

$$\lambda(v_{i,j}, w_{k,l}) = \begin{cases} K(a_i + 1 - j, a_{i+1}, \dots, a_{k-1}, a_k), & k \in \{n-1, n-2\}, \\ K(a_i + 1 - j, a_{i+1}, \dots, a_{k-1}, l), & k = n. \end{cases}$$

□

Theorem 3.80. (Generalised Ptolemy relation.) Let V and W be nice triangles such that the slices between each pair of vertices, one from V and one from W , contain at least one tetrahedron. Then we have

$$P(V, W) = \begin{cases} 1, & \text{if } V \text{ is a right triangle,} \\ 0, & \text{if } V \text{ is a left triangle.} \end{cases}$$

Proof. Let us first consider the case $P(\triangle_R, \triangle_R)$. Assume that the exponential form of the LR sequence for the polyhedron defined by the two triangles is (a_1, \dots, a_n) , so the determinant matrix of λ -lengths is

$$P(\triangle_R, \triangle_R) = \begin{pmatrix} K(a_3, \dots, a_n) & K(a_3, \dots, a_{n-1}) & K(a_3, \dots, a_{n-1}) \\ K(a_1, \dots, a_n) & K(a_1, \dots, a_{n-1}) & K(a_1, \dots, a_{n-1}) \\ K(a_1 - 1, \dots, a_n) & K(a_1 - 1, \dots, a_{n-1}) & K(a_1 - 1, \dots, a_{n-1}) \end{pmatrix}.$$

Recall from Proposition 3.65 that the matrix $M_n(a_1, \dots, a_n)$ has determinant 1. We define two matrices M_{Row} and M_{Col} by

$$M_{\text{Row}} = \begin{pmatrix} 0 & 1 & -a_1 \\ 1 & 0 & 0 \\ 1 & 0 & -1 \end{pmatrix}, \quad M_{\text{Col}} = \begin{pmatrix} 1 & 1 & 0 \\ 0 & -1 & 1 \\ 0 & -1 & 0 \end{pmatrix}.$$

Then we have that

$$P(\triangle_R, \triangle_R) = M_{\text{Row}} \cdot M_n(a_1, \dots, a_n) \cdot M_{\text{Col}}.$$

Since $\det(M_{\text{Row}}) = \det(M_{\text{Col}}) = 1$ we have that $\det(P(\triangle_R, \triangle_R)) = 1$. A similar computation shows that $\det(P(\triangle_R, \triangle_L)) = 1$. Consider now the case

$$P(\triangle_L, \triangle_R) = \begin{pmatrix} K(a_1, \dots, a_n) & K(a_1, \dots, a_n - 1) & K(a_1, \dots, a_{n-1}) \\ K(a_2, \dots, a_n) & K(a_2, \dots, a_n - 1) & K(a_2, \dots, a_{n-1}) \\ K(a_1 - 1, \dots, a_n) & K(a_1 - 1, \dots, a_n - 1) & K(a_1 - 1, \dots, a_{n-1}) \end{pmatrix}.$$

Using the recursion formula of continuants we see that Row 1 = Row 2 + Row 3, and hence $\det(P(\triangle_L, \triangle_R)) = 0$. Similarly we observe that $\det(P(\triangle_L, \triangle_L)) = 0$. \square

Remark 3.81. It is not clear what happens when there are zero elements.

3.7.3 Frieze pattern in higher dimensions

We conclude this subsection with the following topological definition of frieze pattern in three dimensions.

Definition 3.82. Consider a Farey polyhedron P and with prismatic diagram D , let $V(D)$ be the set of vertices of D . Consider the function

$$\lambda : V(D) \times V(D) \rightarrow \mathbb{Z},$$

whose values on two vertices is the λ -length between the corresponding vertices in the Farey polyhedron. We call the collection $(\partial D \times \partial D, \lambda)$ the *frieze pattern* associated to the given Farey polyhedron.

Remark 3.83. In the two-dimensional case this definition will coincide with the classical one once we replace ∂D with its universal covering. In higher dimensional case we propose to follow the diagram ∂D itself for the sake of transparency.

As we have discussed above the frieze pattern satisfies the Ptolemy relation for pairs of faces in the prismatic diagram. Let us illustrate this by the following example.

Example 3.84. Consider a continued fraction

$$[3; 1 : 2 : 1 : 2 : 3 : 3 : 1]$$

with marked faces $V = v_{2,1}v_{2,2}v_{1,4}$ and $W = v_{7,2}v_{7,3}v_{5,3}$ as in Figure 6. The geodesic $\ell(V, W)$ has exponential LR sequence $(1, 2, 1, 2, 3, 2)$. The pairwise vertices are as follows

$$\begin{aligned} P(V, W) &= \begin{pmatrix} K(a_1, \dots, a_n) & K(a_1, \dots, a_{n-2}) & K(a_1, \dots, a_{n-1}) \\ K(a_1 - 1, \dots, a_n) & K(a_1 - 1, \dots, a_{n-2}) & K(a_1 - 1, \dots, a_{n-1}) \\ K(a_3, \dots, a_n) & K(a_3, \dots, a_{n-2}) & K(a_3, \dots, a_{n-1}) \end{pmatrix} \\ &= \begin{pmatrix} K(1, 2, 1, 2, 3, 2) & K(1, 2, 1, 2) & K(1, 2, 1, 2, 3, 1) \\ K(0, 2, 1, 2, 3, 2) & K(0, 2, 1, 2) & K(0, 2, 1, 2, 3, 1) \\ K(1, 2, 3, 2) & K(1, 2) & K(1, 2, 3, 1) \end{pmatrix} \\ &= \begin{pmatrix} 218 & 21 & 112 \\ 105 & 10 & 54 \\ 41 & 4 & 21 \end{pmatrix}. \end{aligned}$$

In particular $\det P(V, W) = 1$.

Remark 3.85. Informally speaking there is a certain similarity between the structure of multidimensional frieze patterns and Voronoi continued fractions introduced in [50]: here one constructs a special polyhedron and writes elementary matrix transitions between its faces. The construction of the Voronoi polyhedra are substantially different. The question of establishing the link between Voronoi continued fractions and multidimensional frieze patterns is open.

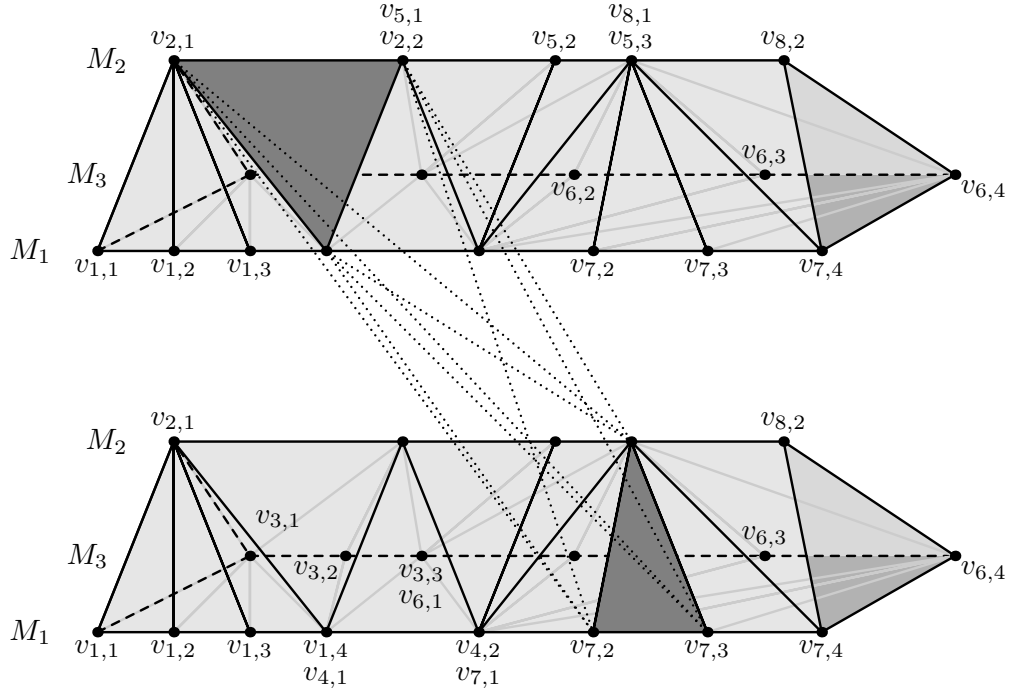


Figure 6: Prismatic diagram for $[3; 1 : 2 : 1 : 2 : 3 : 3 : 1]$.

4 Suggestions for further work

We conjecture that the construction in this paper has a natural extension to other subtractive algorithms and the multidimensional subtractive algorithms as well. From this we propose the following open problems for further study.

Problem 2. Describe the edge sail duality in the higher dimensional case ($n \geq 4$). Here corresponding tables similar to Table 1 in the three-dimensional case may be built.

Problem 3. What is the analogue of nose stretching for other algorithms. What are their geometric properties.

Problem 4. Extend the theory of Farey simplices and their sails to other subtractive algorithms.

Problem 5. Compare the properties of different subtractive algorithms and their characteristic features.

Problem 6. Study the frieze pattern defined by prismatic diagrams in three dimensions and above.

Acknowledgment: The second author is supported by EPSRC grant EP/W002817/1.

References

- [1] V. I. Arnold. *Continued fractions (In Russian)*. Moscow: Moscow Center of Continuous Mathematical Education, 2002.

- [2] V. I. Arnold. “Higher-dimensional continued fractions”. *Regul. Chaotic Dyn.* 3.3 (1998). J. Moser at 70 (Russian), pp. 10–17.
- [3] S. Assaf et al. “A dual approach to triangle sequences: a multidimensional continued fraction algorithm”. *Integers* 5.1 (2005), A8, 39.
- [4] I. Assem, G. Dupont, R. Schiffler, and D. Smith. “Friezes, strings and cluster variables”. *Glasgow Math. J.* 54.1 (2012), pp. 27–60.
- [5] O. R. Beaver and T. Garrity. “A two-dimensional Minkowski $\varphi(x)$ function”. *J. Number Theory* 107.1 (2004), pp. 105–134.
- [6] V. Berthé, L. Lhote, and B. Vallée. “The Brun gcd algorithm in high dimensions is almost always subtractive”. *J. Symbolic Comput.* 85 (2018), pp. 72–107.
- [7] J. Blackman, O. Karpenkov, and J. Dolan. “Multidimensional integer trigonometry”. *Commun. Math.* 31.2 (2023), pp. 1–26.
- [8] K. Briggs. *Klein polyhedra*, <http://keithbriggs.info/klein-polyhedra.html>.
- [9] V. Brun. “Algorithmes euclidiens pour trois et quatre nombres”. *Treizième congrès des mathématiciens scandinaves, tenu à Helsinki 18-23 août 1957*. Mercators Tryckeri, Helsinki, 1958, pp. 45–64.
- [10] A. D. Bryuno and V. I. Parusnikov. “Klein polyhedra for two Davenport cubic forms”. *Math. Notes* 56.3-4 (1995). Russian version: *Mat. Zametki*, 56(4), 1994, 9–27, pp. 994–1007.
- [11] P. Caldero and F. Chapoton. “Cluster algebras as Hall algebras of quiver representations”. *Comment. Math. Helv.* 81.3 (2006), pp. 595–616.
- [12] J. Conway and H. S. M. Coxeter. “Triangulated polygons and frieze patterns”. *Math. Gaz.* 57 (1973), pp. 87–94, 175–183.
- [13] H. S. M. Coxeter. “Frieze patterns”. *Acta Arith.* 18 (1971), pp. 297–310.
- [14] T. Garrity. “On periodic sequences for algebraic numbers”. *J. Number Theory* 88.1 (2001), pp. 86–103.
- [15] O. N. German. “Sails and Hilbert bases”. *Proc. Steklov Inst. Math.* 239.4 (2002). Russian version: *Tr. Mat. Inst. Steklova*, (4)239, 2002, 98–105, pp. 88–95.
- [16] O. N. German and E. L. Lakshtanov. “On a multidimensional generalization of Lagrange’s theorem for continued fractions”. *Izv. Math.* 72.1 (2008). Russian Version: *Izv. Ross. Akad. Nauk Ser. Mat.*, 72(1), 2008, 51–66, pp. 47–61.
- [17] D. J. Grabiner. “Farey nets and multidimensional continued fractions”. *Monatsh. Math.* 114.1 (1992), pp. 35–61.
- [18] D. M. Hardcastle and K. Khanin. “On almost everywhere strong convergence of multidimensional continued fraction algorithms”. *Ergodic Theory Dynam. Systems* 20.6 (2000), pp. 1711–1733.
- [19] A. Hurwitz. “Ueber die angenäherte Darstellung der Zahlen durch rationale Brüche”. *Math. Ann.* 44.2-3 (1894), pp. 417–436.
- [20] C. G. J. Jacobi. “Allgemeine Theorie der Kettenbruchähnlichen Algorithmen, in welchen jede Zahl aus drei vorhergehenden gebildet wird (Aus den hinterlassenen Papieren von C. G. J. Jacobi mitgetheilt durch Herrn E. Heine)”. *Journal für die Reine und Angewandte Mathematik* 69.1 (1868), pp. 29–64.

- [21] O. Karpenkov. “Elementary notions of lattice trigonometry”. *Mathematica Skandinavica* 102 (2008), pp. 161–205.
- [22] O. Karpenkov. *Geometry of Continued Fractions*. Second. Vol. 26. Algorithms and Computation in Mathematics. Springer, Berlin, 2022, pp. xx+451.
- [23] O. Karpenkov. “On a periodic Jacobi-Perron type algorithm”. *To appear in Monatshefte für Mathematik*; *arXiv:2101.12627, preprint* (2024).
- [24] O. Karpenkov. “On Hermite’s problem, Jacobi-Perron type algorithms, and Dirichlet groups”. *Acta Arith.* 203.1 (2022), pp. 27–48.
- [25] O. Karpenkov. “On the triangulations of tori associated with two-dimensional continued fractions of cubic irrationalities”. *Funct. Anal. Appl.* 38.2 (2004). Russian version: *Funkt. Anal. Prilozh.* 38 (2), 2004, 28–37, pp. 102–110.
- [26] O. Karpenkov. “Three examples of three-dimensional continued fractions in the sense of Klein”. *C. R. Math. Acad. Sci. Paris* 343.1 (2006), pp. 5–7.
- [27] O. Karpenkov, F. Mohammadi, C. Müller, and B. Schulze. *Klein-Arnold tensegrities, preprint*.
- [28] A. Ya. Khinchin. *Continued fractions*. Moscow, FISMATGIS, 1961.
- [29] F. Klein. “Sur une représentation géométrique de développement en fraction continue ordinaire”. *Nouv. Ann. Math.* 15.3 (1896), pp. 327–331.
- [30] F. Klein. “Ueber eine geometrische Auffassung der gewöhnliche Kettenbruchentwicklung”. *Nachr. Ges. Wiss. Göttingen Math-Phys. Kl.* 3 (1895), pp. 352–357.
- [31] M. L. Kontsevich and Yu. M. Suhov. “Statistics of Klein polyhedra and multidimensional continued fractions”. *Pseudoperiodic topology*. Vol. 197. Amer. Math. Soc. Transl. Ser. 2. Providence, RI: Amer. Math. Soc., 1999, pp. 9–27.
- [32] E. I. Korkina. “The simplest 2-dimensional continued fraction”. *J. Math. Sci.* 82.5 (1996). *Topology*, 3, pp. 3680–3685.
- [33] E. I. Korkina. “Two-dimensional continued fractions. The simplest examples”. *Trudy Mat. Inst. Steklov* 209.Osob. Gladkikh Otobrazh. s Dop. Strukt. (1995), pp. 143–166.
- [34] C. Kraaikamp and R. Meester. “Ergodic properties of a dynamical system arising from percolation theory”. *Ergodic Theory Dynam. Systems* 15.4 (1995), pp. 653–661.
- [35] G. Lachaud. “Polyèdre d’Arnol’d et voile d’un cône simplicial: analogues du théorème de Lagrange”. *C. R. Acad. Sci. Paris Sér. I Math.* 317.8 (1993), pp. 711–716.
- [36] R. W. J. Meester. “An algorithm for calculating critical probabilities and percolation functions in percolation models defined by rotations”. *Ergodic Theory Dynam. Systems* 9.3 (1989), pp. 495–509.
- [37] R. W. J. Meester and T. Nowicki. “Infinite clusters and critical values in two-dimensional circle percolation”. *Israel J. Math.* 68.1 (1989), pp. 63–81.
- [38] F. Mohammadi and X. Wu. “Rational tensegrities through the lens of toric geometry”. *Comput. Geom.* 119 (2024), Paper No. 102075, 8.
- [39] S. Morier-Genoud. “Coxeter’s frieze patterns at the crossroads of algebra, geometry and combinatorics”. *Bulletin of the London Mathematical Society* 47.6 (2015), pp. 895–938.
- [40] S. Morier-Genoud and V. Ovsienko. “Farey Boat: Continued Fractions and Triangulations, Modular Group and Polygon Dissections”. *Jahresber. Dtsch. Math.* 121 (2019), pp. 91–136.

- [41] J.-O. Moussaïfir. “Sails and Hilbert bases”. Russian, with Russian summary. *Funct. Anal. Appl.* 34.2 (2000). Russian version: *Funkt. Anal. Prilozh.* 34, (2) 2000, 43–49, pp. 114–118.
- [42] G. Panti. “Multidimensional continued fractions and a Minkowski function”. *Monatsh. Math.* 154.3 (2008), pp. 247–264.
- [43] V. I. Parusnikov. “Klein polyhedra for the fourth extremal cubic form”. *Math. Notes* 67.1-2 (2000). Russian version: *Mat. Zametki*, 67(1),2000), 110–128, pp. 87–102.
- [44] O. Perron. “Erweiterung eines Markoffschen Satzes über die Konvergenz gewisser Kettenbrüche”. *Math. Ann.* 74.4 (1913), pp. 545–554.
- [45] O. Perron. “Grundlagen für eine Theorie des Jacobischen Kettenbruchalgorithmus”. *Math. Ann.* 64.1 (1907), pp. 1–76.
- [46] E. V. Podsypanin. “A generalization of the continued fraction algorithm that is related to the Viggo Brun algorithm”. *Zap. Nauchn. Sem. Leningrad. Otdel. Mat. Inst. Steklov. (LOMI)* 67 (1977). *Studies in number theory (LOMI)*, 4, pp. 184–194, 227.
- [47] F. Schweiger. *Multidimensional continued fractions*. Oxford Science Publications. Oxford University Press, Oxford, 2000, pp. viii+234.
- [48] I. Short. “Classifying SL_2 -tilings”. *Trans. Amer. Math. Soc.* 376 (2022), pp. 1–38.
- [49] H. Tsuchihashi. “Higher-dimensional analogues of periodic continued fractions and cusp singularities”. *Tohoku Math. J. (2)* 35.4 (1983), pp. 607–639.
- [50] G. F. Voronoi. “On a generalization of the algorithm of continued fractions, Doctoral dissertation.” *Warsaw (in Russian)* (1896).
- [51] G. K. White. “Lattice tetrahedra”. *Canadian J. Math.* 16 (1964), pp. 389–396.